AD_____

Award Number: DAMD17-99-1-9571

TITLE: Molecular Mechanisms of Soft Tissue Regeneration and Bone
       Formation in Mice: Implications in Fracture Repair and
       Wound Healing in Humans

PRINCIPAL INVESTIGATOR: David J. Baylink, M.D.

CONTRACTING ORGANIZATION: Loma Linda Veterans Association for
                             Research and Education
                           Loma Linda, California 92357

REPORT DATE: October 2002

TYPE OF REPORT: Annual

PREPARED FOR: U.S. Army Medical Research and Materiel Command
               Fort Detrick, Maryland 21702-5012

DISTRIBUTION STATEMENT: Approved for Public Release;
                         Distribution Unlimited

The views, opinions and/or findings contained in this report are
those of the author(s) and should not be construed as an official
Department of the Army position, policy or decision unless so
designated by other documentation.

REPORT DOCUMENTATION PAGE

Form Approved
OMB No. 074-0188

Public reporting burden for this collection of information is estimated to average 1 hour per response, including the time for reviewing instructions, searching existing data sources, gathering and maintaining the data needed, and completing and reviewing this collection of information. Send comments regarding this burden estimate or any other aspect of this collection of information, including suggestions for reducing this burden to Washington Headquarters Services, Directorate for Information Operations and Reports, 1215 Jefferson Davis Highway, Suite 1204, Arlington, VA 22202-4302, and to the Office of Management and Budget, Paperwork Reduction Project (0704-0188), Washington, DC 20503

1. AGENCY USE ONLY (Leave blank)	2. REPORT DATE October 2002	3. REPORT TYPE AND DATES COVERED Annual (1 Oct 01 – 30 Sep 02)

4. TITLE AND SUBTITLE
Molecular Mechanisms of Soft Tissue Regeneration and Bone Formation in Mice: Implications in Fracture Repair and Wound Healing in Humans

5. FUNDING NUMBERS
DAMD17-99-1-9571

6. AUTHOR(S):
David J. Baylink, M.D.

7. PERFORMING ORGANIZATION NAME(S) AND ADDRESS(ES)

Loma Linda Veterans Association for
   Research and Education
Loma Linda, California 92357

E-Mail: baylid@lom.med.va.gov

8. PERFORMING ORGANIZATION REPORT NUMBER

9. SPONSORING / MONITORING AGENCY NAME(S) AND ADDRESS(ES)

U.S. Army Medical Research and Materiel Command
Fort Detrick, Maryland 21702-5012

10. SPONSORING / MONITORING AGENCY REPORT NUMBER

11. SUPPLEMENTARY NOTES

12a. DISTRIBUTION / AVAILABILITY STATEMENT
Approved for Public Release; Distribution Unlimited

12b. DISTRIBUTION CODE

13. Abstract *(Maximum 200 Words)* *(abstract should contain no proprietary or confidential information)*

The primary goal of the proposed work is to identify genes which play an anabolic role in bone and soft tissue function and to clarify the function of these genes. Three hypotheses have been proposed:1) the high bone density gene in chromosome 1 in our CAST/B6 congenic mice can be clones; 2) Genes that regulate soft-and hard-tissue regeneration can be identified by using appropriate mouse strains that exhibit differences in regeneration; and 3) ENU mutagenesis, applied to our mouse model, will lead to the identity of genes that regulate soft and hard tissue function. During the last funding period, we have proposed several specific objectives for each of the above mentioned hypothesis. As disclosed in the progress report, we have successfully accomplished all of the specific objectives. Our work during this reporting period has resulted in three published manuscripts, one manuscript in press, one submitted manuscript, one manuscript under revision for publication, and two abstracts. We believe that successful accomplishment of the proposed studies will provide a better understanding of the molecular mechanisms involved in hard- and soft-tissue regeneration and will provide a framework for future development of therapies for hard and soft tissue injuries.

14. SUBJECT TERMS
soft and hard tissue regeneration, bone density, gene function, mouse genetics, cDNA microarray analysis, congenic mice, QTL analysis, musculoskeletal genes

15. NUMBER OF PAGES
54

16. PRICE CODE

17. SECURITY CLASSIFICATION OF REPORT Unclassified	18. SECURITY CLASSIFICATION OF THIS PAGE Unclassified	19. SECURITY CLASSIFICATION OF ABSTRACT Unclassified	20. LIMITATION OF ABSTRACT Unlimited

NSN 7540-01-280-5500

Standard Form 298 (Rev. 2-89)
Prescribed by ANSI Std. Z39-18
298-102

Table of Contents

General Introduction

The primary goal of the project funded by the U.S. Army is to identify genes which play an anabolic role in bone tissue and soft tissue function, particularly during regeneration, and to clarify the function of these genes. To accomplish this goal, we have proposed 3 technical objectives during the funding period. These 3 technical objectives are as follows:

1. Studies proposed in the first technical objective are designed to employ state-of-the-art molecular biotechniques to identify the gene located in mouse chromosome 1 that is involved in the regulation of peak bone density.

2. Our second technical objective has been focused on identifying the key genes that are involved in soft tissue repair/regeneration using inbred strains of mice as model systems.

3. The goal of our third technical objective is to identify and characterize novel genes, using ENU mutagenesis techniques and to elucidate the function of known genes that play a key role in the metabolism of bone and soft tissue.

Our goals for the last 12-months of the second funding period for each of the technical objectives, as well as our progress for each of the technical objectives, are described below. The progress report for each technical objective is organized according to the outline provided by the office of the U.S. Army Medical Research and Materiel Command.

A. Technical Objective 1: Positional clone the QTL gene that controls bone density on mouse chromosome 1.

1. Introduction

Our ultimate objective is to clone the QTL gene regulating peak bone density on chromosome 1 in the CAST/B6 congenic mice by the application of cDNA microarray, followed by positional candidate gene functional studies. This report includes our progress for the last twelve months of the current proposal.

Our studies are designed to employ state-of-the-art molecular biotechniques to identify the gene located in chromosome 1 that is involved in the regulation of peak bone density. The molecular approaches that we proposed to undertake include: a) Fine mapping of the quantitative trait loci (QTL) region by developing subcongenic lines of mice which contain the QTL region; b) Selection of candidate genes by differences in gene expression by microarray approach; c) Identification of candidate genes in the known DNA sequences of human genome that are syntenic to QTL region in mouse chromosome 1; and d) Construction of BAC clone contig that covers the QTL region of chromosome 1 to aid in the identification of bone density gene.

Our specific objectives during the last 12 months of this grant period were as follows:

a) To develop and characterize the subcongenic strains which contain the QTL region

b) To complete the analysis of gene expression experiments using commercial and in house microarray assay and search for candidate genes.

c) To evaluate if BAC fragments could be used as probes to identify differentially expressed genes between sub congenic and B6 mice.

d) To initiate sequencing of BAC fragment for which syntenic human DNA sequences are not available and that is differentially expressed in the bones of congenic and B6 mice.

Our progress in each of the specific objectives is given below.

2. Body
Specific Objectives For The Last Twelve Months Of The Second Funding Period
a)   Specific Objective 1: To develop and characterize the subcongenic strains that contain the QTL region.

In order to accomplish this objective, we successfully developed and characterized subcongenic strains that confirmed the hypothesis we made in our previous annual report regarding the position of the QTL.

Using the subcongenic created during the first six months of this grant, we prepared new subcongenic strains that confirmed the position of the QTL between the markers D1mit540 and D1mit221. In our last report, we presented data on the subcongenic strains, designated B6.CAST-1-2, 1-3, 1-11, 1-12 (Fig. 1), which contained the BMD QTL with CAST alleles, while the rest of the genome was B6 in composition. Our initial analysis indicated that there was no significant difference in body weight or in the length of femora between the congenic and the B6 mice, while the total BMD of the femur of the congenic mice was significantly greater than that of B6 mice (1, 2). Here we report the follow-up analysis of the BMD phenotypes for the previous and the new subcongenic strains B6-CAST-1-13, -1-14, -1-15.

To produce new subcongenic strains, we crossed the previous subcongenic female B6.CAST-1-11 (N8) mice with the male B6 (N4) mice to produce the heterozygot F1 mice. Next, F2 mice were produced by intercrossing F1 mice. The progenies were genotyped in the QTL region. Individuals with a crossover genotype between B6 and CAST in the QTL region were selected for further crosses. Finally, progenies with smaller chromosomal region from CAST were intercrossed to produce homozygous subcongenic lines.

Three new subcongenic B6.CAST-1-13, -1-14, and-1-15 were produced and bred for homozygosity, in addition to the nine subcongenic strains reported last year, B6.CAST-1-1 to to -7, and B6.CAST-1-10 to –12 . These covered different portions of the original QTL region and overlapped with each other (Figure 1).

The sizes of the CAST chromosome in different subcongenic strains shown in Figure 1 were determined by molecular markers. The initial B6.CAST-1T congenic strain contains a chromosomal region from *D1mit14* to *D1mit17* on Chr. 1 from CAST. In order to breed subcongenic lines, 21 markers were eventually selected for our genotyping. Table 1 lists the molecular markers that we used in genotyping the subcongenic strains. For genotyping, PCR-based genotyping with microsatellite markers was performed, as described previously (1, 2). DNA from F_2 progenies of subcongenic strains and B6 mice was extracted from either a piece of tissue from ear punch or a tail tip using the QIAamp Tissue Kit (Qiagen, Chatsworth, CA). PCR was conducted on a DNA engine tetrad from MJ Research Inc. (Watertown, MA). PCR products were separated in 7% polyacrylamide gel and visualized with Ethidium Bromide under UV light.

Because our initial analysis during the last funding period indicated that 16 weeks of age is the best time for measurement of bone density, we obtained femurs from subcongenic strains and B6 mice at 16 weeks of age. The inbred mouse strain, B6, was obtained from The Jackson Laboratory (JAX). Subcongenic strains were produced and maintained in the research colony under 14:10 hr. light:dark cycle in the J. L. Pettis Memorial VA Medical Center (JLPMVAMC) and in JAX. An autoclaved diet of NIH-31 with 6% fat and HCl-acidified water (pH 2.8-3.2) was available at all times. All animal protocols were reviewed and approved by the Institutional Animal Care and Use Committees of the JAX and of the Jerry L. Pettis Memorial V.A. Medical Center.

Table 1. Molecular Markers Along The QTL Region Used In Congenic Breeding

| Marker Name	Size in CAST (bp)	Size in B6 (bp)	Approximate Position (cM)
D1MIT14	196	180	81.5
D1Mit268	107	131	83.40
D1Mit106	94	120	85.00
D1MIT57	272	207	87.80
D1MIT453	84	96	89.40
D1MIT112	188	180	91.30
D1MIT111	202	170	92.3
D1Mit113	224	206	93.30
D1Mit540	91	127	95.8
D1MIT356	112	152	95.8
D1Mit355	104	112	97.0
D1mit541	116	126	97.7
D1MIT115	124	148	99.7
D1Mit403	195	125	100.0
D1Mit37	94	124	101.0
D1Mit151	124	108	101.0
D1Mit406	135	125	101.2
D1MIT360	100	116	101.2
D1Mit221	115	132	102.0
D1MIT459	97	117	102.0
D1MIT17	190	170	106.3
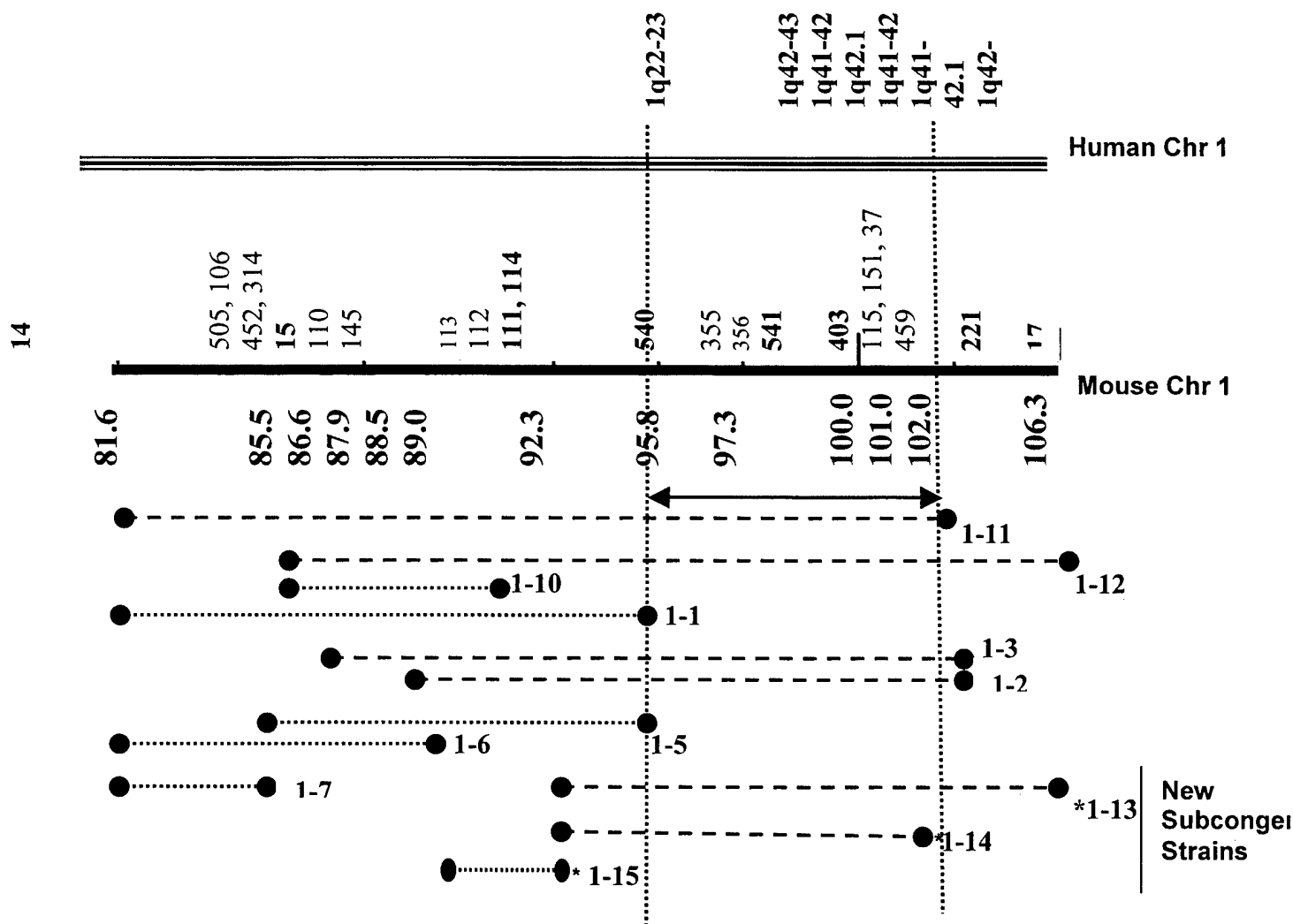
Figure 1. Subcongenic Lines of the QTL Region. 1) On the top is human chromosome 1. The triple line and the map positions indicated above the triple line represent the homologous regions on human Chr 1 to mouse chromosome 1. 2) In the middle is the map of mouse chromosome 1. The solid bar represents the original region of Chr 1 from CAST within the congenic strain B6.CAST-1. Numbers above the solid bar represent the position and names of D1mit microsatellite markers, while the number under the solid bar represents the cM distance on mouse Chr 1. 3) At the bottom are the subcongenic strains for the QTL locus of bone density on mouse chromosome 1. The dashed lines represent the chromosomal regions covered by the six subcongenic strains that contain the QTL gene. The dotted lines represent the region covered by each of the six subcongenic strains that did not contain the QTL gene. The region indicated by the solid two-headed arrow between the two vertical lines is the proposed QTL region, based on information of BMD of subcongenic strains. The region indicated by a dotted two-headed arrow indicate a possible QTL region based on chromosomal location of BMD QTLs in mice and humans. *New subcongenic strains; the 1-13 and the 1-14 subcongenic showed high BMD, however the 1-15 subcongenic showed no significant difference with the B6 mice.

We measured the total bone density, cortical density of each subcongenic strain and the B6 mice. Femoral total BMD was measured by peripheral quantitative computerized tomography (pQCT) with a Stratec XCT 960M (Norland Medical Systems, Ft. Atkinson, WI), as previously described (1).

ANOVA was performed to evaluate the statistical significance of differences in the BMD values between subcongenic and the B6 strain. Values were expressed as Mean±SE; differences at $P < 0.05$ were considered as significant.

The BMD phenotype for the first nine subcongenic has been reported in our last report where we suggested that the QTL should be on the region between the markers D1mit540 and D1mit221. As for the new subcongenic, at 16 weeks the cortical density of the B6.CAST-1-13 was significantly higher than that of the recipient strains, confirming the position of the QTL in the CAST segment. The BMD for B6.CAST1-1-15 was similar to that of B6 mice, suggesting that it doesn't have the CAST alleles for the QTL gene.
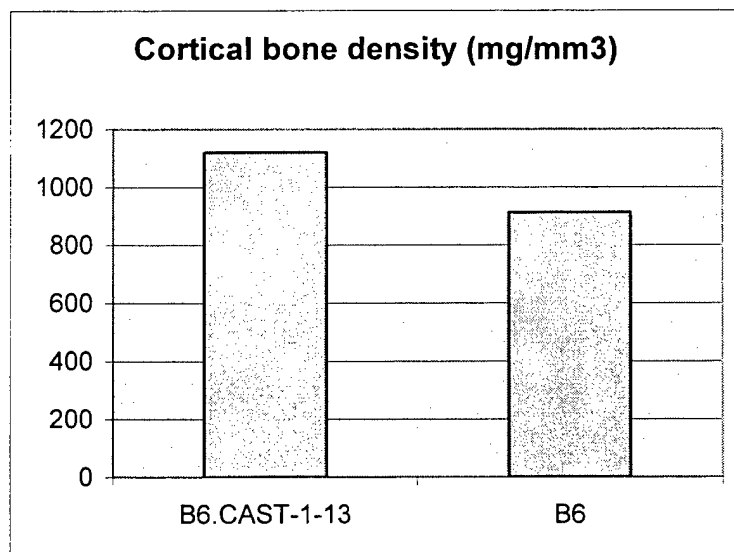

Figure 2: BMD of the B6.CAST-1-13 compared to that of the wild type B6.

In addition, by examining the BMD of different genotypes in male and female congenic mice, we found interesting information concerning the biological mechanism and genetic effect of this *cast* allele on BMD of male and female mice.

By analysis of BMD of female mice in an F_2 population, we had previously found that the inheritance pattern of this QTL locus was additive (1). In order to investigate the gender effect of this QTL, we compared the BMD among the homozygous *cast/cast* genotype (from B6.CAST-1-10 and B6.CAST-1-11), the heterozygous *cast/b6* genotype (from B6.CAST-1-10), and the homozygous *b6/b6* of male, as well as in female mice, shown in Figure 3.

We found that the heterozygous *cast/b6* genotype did not increase the BMD in the male mice (0.617±0.005 mg/mm^3 vs. 0.620±0.003mg/mm^3), suggesting the *b6* allele is

. dominant to the *cast* allele in the male mice. Considering the differences in BMD among the three genotypes, *cast/cast*, *cast/b6*, and *b6/b6* (0.653±0.007mg/mm^3, 0.617±0.005mg/mm^3, 0.620±0.003mg/mm^3, respectively), we believe that the *cast* allele was recessive to *b6* allele in the male mice.

Conversely, the total femoral BMD of *cast/b6* genotype increased 4% in female mice (0.641±0.003 mg/mm^3 vs. 0.617±0.005mg/mm^3). ANOVA analysis indicated that the increased level of BMD in *cast/b6* female mice was significantly higher than that of the *b6/b6* genotype (P<0.01), but it was significantly lower than that of the *cast/cast* genotype (0.692±0.008 mg/mm^3 vs. 0.641±0.003mg/mm^3; P<0.01). The phenotype of BMD in *cast/cast* homozygotes was significantly higher than that of heterozygous *cast/b6* (0.692±0.008mg/mm^3 vs. 0.641±0.003mg/mm$^{3)}$ and the heterozygous genotype was significantly higher than that of homozygous *b6/b6* (0.641±0.003mg/mm^3 vs. 0.617±0.005mg/mm^3). These results led us to conclude that the *cast* allele is additive to the *b6* allele in female mice.

Accordingly, our results suggested that: 1) the *cast* allele is recessive to the *b6* allele with respect to BMD in male mice; and, conversely, 2) the *cast* allele is dominant (in an additive manner) to the *b6* allele in female mice. These quantitatively phenotypic differences suggested a differential penetration of the QTL gene products between the male and the female mice. Figure 3 shows these differences in BMD between male and female mice.
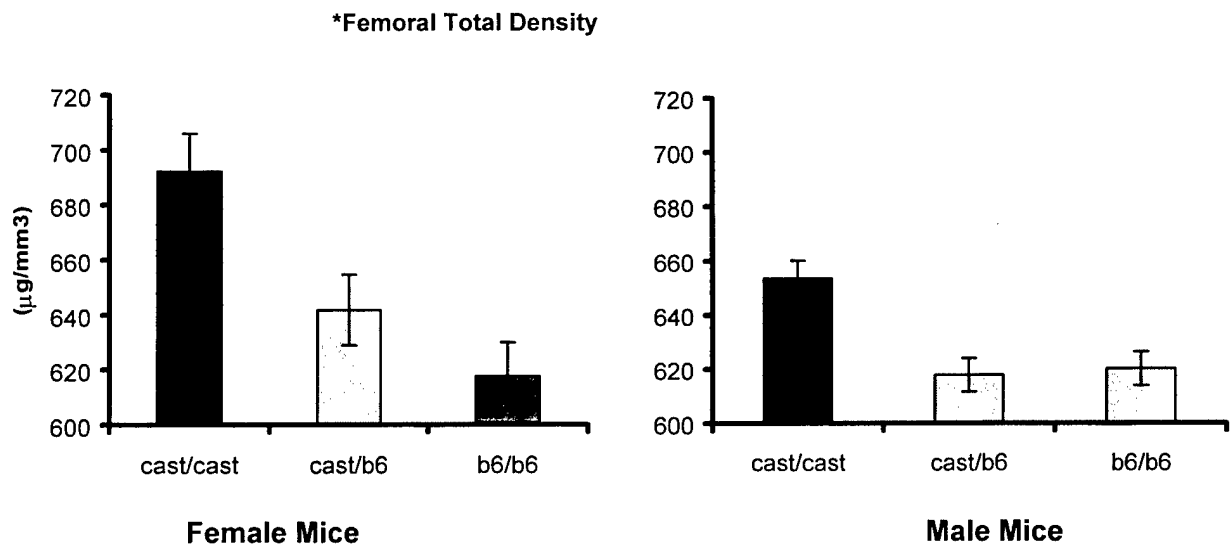
*Femoral Total Density

Figure 3. *Effect of a Different Genotype of the QTL Gene on BMD. BMD of homozygous cast/cast genotype are significantly higher, statistically, than that of b6/b6 genotype (*For total density in female and in male mice, ANOVA analysis showed *P value <0.001 between cast/cast genotype and b6/b6 genotype). Heterozygous (cast/b6) genotype increased total BMD of mouse femurs in female mice (**P=0.01) but not in male mice. There is no statistically significant difference between BMD in heterozygous cast/b6 female mice and homozygous cast/cast male mice.*

*P value <0.001 between cast/cast genotype and b6/b6 genotype). Heterozygous (cast/b6) genotype increased total BMD of mouse femurs in female mice (**P=0.01) but not in male mice.

Page 9

Our subcongenic approach not only confirmed the biological activity of the QTL gene in this region, but also further narrowed the size of the QTL locus within Chr 1. Figure 1 shows the fine mapping of this QTL locus by comparison of molecular markers among twelve subcongenic strains. Previously, we showed that the size of this QTL region was about 25 cM (1, 2). Comparison of the marker locations in the nine subcongenic strains plus the new ones; the B6-CAST-1-13 and B6-CAST-1-14 found that the six strains that had a high BMD contained a common region from 95.8 to 102 cM (between *D1Mit540* and *D1Mit221*). This region was not included in any of the other six low BMD subcongenic strains. Thus, it allowed us to further map the QTL locus to an approximate 7 cM region (Figure 1) on mouse Chr 1. We also included the human homologous region on chromosome 1 in Figure 1.

b.   Specific objective 2: To complete the analysis of gene expression experiments using commercial and in-house microarray assays and to search for cancidate genes.

We selected the candidate genes by comparing the results of commercial microarray and in-house microarray. We identified the genes located in the human genome that are syntenic to the QTL region on mouse chromosome 1 and evaluated their known functions. In addition, we identified the open reading frame of known DNA sequences of the human genome that are syntenic to the QTL region on mouse chromosome 1 for future studies with the positional candidate genes approach.

For gene expression studies using microarray, six week-old and fourteen week-old female B6 and B6.CAST-1 mice were used in this study. We used three different tissues (femur, liver and spleen) in order to identify potential genes for bone formation.

With a threshold of 800 relative units, which corresponds to the average of 5 replicates of the negative control mean signal value plus 2 times the standard deviation, 80% of the genes on the chips showed a detectable hybridization with cDNA from femur of 14 week-old mice and 72% hybridized with cDNA from femur of 6 week-old mice. Some of this data, as well as the list of the genes used at our in-house microarray, have been reported on in last year's report. We compared the gene expression pattern between the congenic and the B6 mice in order to identify candidate genes for bone density. The criteria for a significant differential expression were that both the data from commercial and in-house microarray agreed and the results could be duplicated. In addition, of the bone formation genes reported in the previous report, we have found 3 ESTs and 3 known genes that were differentially expressed between the congenic mice and the control mice (Table 2 and 3). These genes will be further analyzed to identify their potential function within bone.

In our previous reports, we stated that the C-reactive was the only known gene in mouse BMD QTL region that showed differential expression between B6 and the congenic mice. The human syntenic gene was also present in the corresponding syntenic region of chromosome 1.

Table 2: ESTs up-regulated in the femur from the congenic mice (data from commercial microarray and in-house microarray:

Gene ID.	Expression ratio in Femur 14 weeks Cong/B6	Expression ratio in Femur 6 weeks Cong/B6	Function	Reference
ESTs. highly similar to Mus musculus diadenosine triphosphate hydrolase (Fhit) gene, intron 5 AA404014	1.5*	3.54	Tumor supressor	Asensio AC. & al., Acta Biochim Pol. 2000;47(2):435-41.
ESTs, AA015542.1	1.57*	3.25	No homology with any known gene	
ESTs AA273950.1	1.76*	2.6	–	–

*same results as from commercial microarray

Table 3: Genes and ESTs up-regulated in Femur from The B6 wild type mice:

Gene ID.	Expression ration in Femur 14 weeks Cong/B6[a]	Expression ratio in Femur 6 weeks Cong/B6[b]	Function	Reference
EST {IMAGE:793017} AA437635.1	0.50	0.86	No significant homology with any known gene	-
Mus musculus histone H2A.Z (H2A.Z) mRNA, AA466087.1	0.41	2.9	H2A.Z can positively regulate gene transcription at certain genes under specific cell growth conditions	Adam & al., Mol Cell Biol 2001 Sep;21(18):6270-9
eosinophil-associated ribonuclease 2 AA510161.1	0.44	1.36	likely participate in skin lesion development in Churg-Strauss syndrome	Drage & al., J Am Acad Dermatol 2002 Aug;47(2):209-16

: means that the differential expression is similar to the result achieved from commercial microarray.
: means that the data have been duplicated in-house

c.   Specific Objective 3: The production of congenic strains and subcongenic strains allowed us to narrow down the QTL region. However, in better defining the QTL region, we found that the contig that we had constructed to further narrow down the QTL region was actually outside of the QTL region as determined by the congenic mice data. At this time, we had access to the Celera database, which allowed us to identify all the genes throughout the entire QTL as defined by the subcongenic mice studies. In effect, the Celera database obviated the need to further develop a contig that covers the entire BMD QTL as determined by our congenic data. Therefore, we elected to use the Celera database to construct a specific microarray that would include all of the genes in the QTL as defined by the congenic mice studies. As a result, all of our further work to identify candidate genes in the QTL region shifted away from BAC clones to the production of a specific microarray based on the genes identified in the QTL region by virtue of our Celera database. This shift in the technology to be applied is not a shift in the overall goal to identify candidate genes in the QTL region. Consequently, in our future reporting, we will be reporting on information derived from our in-house microarray designed to include for the most part all the genes in the QTL region based on the Celera database.
Below is our progress in this specific objective:

1- We identified the genes and ESTs in the QTL region using the microsatellites that flank the predicted QTL region, between D1mit450 and D1mit221; 269 probes were identified from celera data (Table 4).
2- We designed primers for every probe: we prepared 2 pair of primer for every probe, the specificity of the primer was checked; the primers were blasted with NCBI and Celara database to be sure that the primer chosen don't hybridize with any other sequence.
3- We extracted Total RNA from Liver and Femur. Then we prepared cDNA using RT-PCR.
4- Optimized the PCR conditions for every pair of primer using cDNA as a template.
5- 200 probes have been amplified and purified. The probes are ready to be mixed with 50% Dimethyl Sulfoxide (DMSO) at 250-300ng/ul final concentration to be spotted on Corning Microarray slides.
6- Because the bone density phenotype is significant at 16 weeks, we decided to use RNA from 16, 14 and 6 week-old mice. We extracted Total RNA, from two of the high bone density subcongenic mice B6.CAST-1-13 and B6.CAST-1-14, with a modified procedure from Life Technologies (Grant Island, NY) using Trizol reagent. The quality of Total RNA was checked by Agilent 2100 Bioanalyzer (Agilent Technologies). The concentration was measured with Spectronic Genesys spectrophotometer. Since we are looking for bone density genes, we used RNA from femur without bone marrow.

d. **Specific Objective 4:** To initiate sequencing BAC fragments, for which synthenic human DNA sequences are not available and that is differentially expressed in the bones of the congenic and B6 mice.

As mentioned above, the BAC portion of our project became unnecessary because the information is now available in the Celera database.

Our progress in this revised objective is as follows:

Because both Mouse sequence and Human sequence are available in the Celera database, we were able to identify mouse genes in the mouse chromosome 1 QTL that are also present in the corresponding syntenic region in human chromosome 1. Based on these data, it appears that 57 genes identified in mouse chromosome 1 QTL are present in the human chromosome 1 BMD QTL (Table 5). The availability of this information will help in establishing priorities for BMD candidate genes for functional studies, since it is likely that the candidate gene for BMD in mouse chromosome 1 QTL and the corresponding Human chromosome 1 QTL are the same.

Table 5: The list of Human synthenic region of the mouse Bone mineral density QTL (known genes and ESTs):

Gene name	Gene symbol	Position in Chr.1mouse QTL (Megabases)	Position in Human chr. 1 (Mbases)	Function as stated by Celera data
Formin 2	Fmn2	178.6	217,2	Cell adhesion
protein related to DAC and cerberus	Prdc-pending	178,9	217,6	Binding protein
regulator of G protein signaling 7	Rgs7	179,15	217,9	Clamodulin binding protein
Fumartae Hydratase		179,70	218,6	Fumartae Hydratase
opsin (encephalopsin)	Opn3	179,75	218,710	Lipoprotein binding
choroideremia-like	Chml	179,77	218,75	RAB proteins GEranylgeranyltransferase
WD Domain Containing Protein		179,85	218,87	Ubiquitin-protein ligase
Exonuclease 1	EXO1	179,96	218,965	Exonuclease 1
Major Envelope related protein related		180,043	219,206	Phospholipase D
Coiled-Coil Protein		180,892	220,218	ATP binding
thymoma viral proto-oncogene 3	Akt3	181,086	220,469	Protein Kinase
zinc finger protein 238	Zfp238	181,509	221,021	Transcription factor
adenylosuccinate	Adss2	181,816	221,37	adenylosuccinate synthetase

synthetase 2				2
Similar to transporter protein, system N1 Na$^+$ and H^{+-} coupled glutamine transporter		182,4	221,820	Ribonucleoprotein
ESTs		182,880	222,659	Unknown
HSKM-B Related		183,019	222,720	DNA binding
house-keeping protein 1		183,598	223,505,	RRNA (adenine-N6,N6-dimethyltransferase)
ESTs		184,228	202,445,366	Chaperone
Preselinin 2	Psen2	184,29	202,53	Enzyme
ESTs		184,40	202,688	1D-myo-inositol-trisphosphate 3-kinase
ADP-ribosyltransferase (NAD+; poly (ADP-ribose) polymerase) 1	Adprt1	184,6	203,02	NAD(+) ADP-ribosyltransferase
Mix1 homeobox-like 1 (Xenopus laevis)	Mixl1	184,756	203,20	transcription factor
Peripheral benzodiazepine receptor associated protein		184,788	203,241	Acyl binding
TRANSFORMING GROWTH FACTOR SUPERFAMILY MEMBER		184,956	203,486	Protein binding
PYRROLINE-5-CARBOXYLATE REDUCTASE		184,967	203,503	PYRROLINE-5-CARBOXYLATE REDUCTASE
TRANSFORMING GROWTH FACTOR BETA-RELATED	Ebah	184,999	203,538	Binding protein
ESTs		185,007	203,545	unkown
epoxide hydrolase 1, microsomal	Ephx1	185,055	203,582,	epoxide hydrolase
NUCLEAR VCP-LIKE PROTEIN		185,16	205,10	ATP binding
ESTs	185,211	205,050		unknown
WD40 REPEAT		185,24	204,99	2-acetyl-1-

PROTEIN				alkylglycerophosphocholine esterase
ESTs		185,409	204,687	unknown
LAMIN B RECEPTOR		185,866	203,997	DNA binding
FATTY ACID DESATURASE-RELATED		186,32	205,23	electron transfer
ESTs		186,358	200,828	Unkown
ANKYRIN-RELATED		186,451	200,410	beta-mannosidase
CALPAIN 2	Capn2	186,509	200,342	calpain
TOLL RECEPTOR-RELATED	Tlr5	187,016	199,789	antibacterial response protein
Patched Rekated		187.1	199.63	glucosylceramidase
Rhophilin-related		187.28	199.40	-
RNA polymerase I		187.39	199.24	Transcription factor
ESTs		187.42	199.21	Uknown
Dual specificity protein phosphatase 8-related	Dusp10	187.99	198.4	Protein phosphatase
Homeobox protein DBX	Hlx	188.69	197.59	Transcription factor
EST		188.84	197.40	Uknown
Protein Kinase sNF1-Realted		188.86	197.24	Protein Kinase
ESTs		189.16	196.86	Unknown
Isolucyl-tRNA synthase		189.24	196.8	ATP binding
PAP-Inositol-1,4-Phosphatase		189.28	196.77	Protein Phosphatase
Glutamyl-tRNA synthetase		189.29	196.68	ATP binding
Zinc transporter SLC30A1-related		189.41	196.62	Serine C-palmitoyltransferase
ESTs		190.03	195.88	Lysophospholipase
Transforming Growth factor beta 2	TGFB2	190.56	195.06	Cell cycle regulator
ESTs		190.66	194.99	Unknown
ESTs		190.98	194.35	Unknown
Tuftelin-interacting protein-related		191.14	194.15	Transcription factor
Estrogen-related receptor gamma		191.92	193.22	Transcription Factor

3. Reportable Outcomes

Full papers:

1. <u>Gu W-K</u>, Li X.M., Donahue L. R., Beamer W.G., Mohan S., Baylink D.J. (2001) A Mouse Database for Genetic Loci That Regulate Bone Density. Bone (MS# AMY-012). Accepted/under revision.
2. <u>Gu W-K</u>, Li X., Lau K-H W., Edderkaoui B., Donahue L., Rosen C.J, Beamer W. G., Shultz K. L., Srivastava A., Mohan S. & Baylink D.J. (2001) Gene expression between a congenic strain that contains a QTL locus of high bone density from CAST/EiJ and its wild type strain C57BL/6j. Functional & Integrative Genomics 2002 Apr;1(6):375-86.
3. <u>Gu W-K</u>, Li X.M., Edderkaoui B., Strong D., Lau K-H.W., Mohan S., & Baylink D. J. (2001) Construction of a BAC contig for a 3 cM biologically significant region of mouse chromosome 1. Genetica 2002;114(1):1-9.

4. Conclusions

We have:

1) Developed a new subcongenic strains which contain shorter regions of the QTL region. These subcongenic are going to be used for in-house microarray in order to identify potential candidate genes that contribute to bone density difference between B6 and CAST mice.
2) We have discovered gender specificity of the BMD QTL.
3) We have identified several known genes and ESTs that are differentially expressed using data from commercial microarray and in-house micorarray. Although many of these known genes and ESTs are not located on the BMD QTL region, they could act downstream to the QTL candidate gene.
4) We prepared 200 probes which represent 75% of the genes and EST located on the QTL region. The probes are going to be mixed with 50% DMSO then spotted on Corning Microarray slide. We will be able to do hybridization and analyze the results
5) We have identified 57 genes that are syntenic between the mouse chromosome 1 QTL and the human chromosome 1. Those syntenic regions are in the Human chromosome 1 BMD QTL (REF?). Because the corresponding syntenic region in Human chromosome 1 also contains a BMD QTL, it is possible that the same gene contributes to BMD difference in both mice and human.

5. References

1. Beamer WG, Shultz KL, Churchill GA, Frankel WN, Baylink DJ, Rosen CJ, Donahue LR. Quantitative trait loci for bone density in C57BL/6J and CAST/EiJ inbred mice. Mamm Genome. 1999 10(11):1043-1049.
2. Gu W, Ray K, Pearce-Kelling S, Baldwin VJ, Langston AA, Ray J, Ostrander EA, Acland GM, Aguirre GD. Evaluation of the APOH gene as a positional candidate for prcd in dogs. Invest Ophthal Visual Sci. 1999 40(6):1229-1237.

3. Koller DL, Econs MJ, Morin PA, Christian JC, Hui SL, Parry P, Curran ME, Rodriguez LA, Conneally PM, Joslyn G, Peacock M, Johnston CC, Foroud T. Genome screen for QTLs contributing to normal variation in bone mineral density and osteoporosis. J Clin Endocrinol Metab. 2000 85(9):3116-3120.

4. Asensio AC, Rodriguez-Ferrer CR, Oaknin S, Rotllan P. Human diadenosine triphosphate hydrolase: preliminary characterisation and comparison with the Fhit protein, a human tumour suppressor. Acta Biochim Pol 2000;47(2):435-41

5. Adam M, Robert F, Larochelle M, Gaudreau L. H2A.Z is required for global chromatin integrity and for recruitment of RNA polymerase II under specific conditions.Mol Cell Biol 2001 Sep;21(18):6270-9

6. Drage LA, Davis MD, De Castro F, Van Keulen V, Weiss EA, Gleich GJ, Leiferman KM. Evidence for pathogenic involvementof eosinophils and neutrophilsin Churg-Strauss syndrome. J Am Acad Dermatol 2002 Aug;47(2):209-16

B.   TECHNICAL OBJECTIVE 2: To identify the key genes involved in soft-tissue repair/regeneration in MRL/MpJ and SJL/J mice.

1.   Introduction

Wound healing involves two major clinical issues: 1) the rate of healing; and 2) the quality of healing. The primary therapeutic goal of the treatment of a wound is to accelerate wound closure with minimal scar formation. However, the success of using therapeutic approaches to treat wounds depends heavily on understanding the molecular mechanisms underlying the wound healing process. The aim of this project is to identify the key genes and their cellular function that regulate the soft- and hard-tissue repair and regeneration in a mouse model.

We proposed the following specific objectives for the final 12 months of the second funding period:

a) To perfom QTL mapping using 300 (MRL/MpJ X SJL/J F2) mice in an attempt to make a linkage map with an even spacing of less than 20 cM between markers.

b) To perform commercial microarray hybridization to identify the differentially expressed genes between MRL/MpJ and SJL/J.

c) To build a knowledge-based microarray chip that will include growth factors and other important regulatory genes known to be involved in soft tissue repair/regeneration and the genes that are localized in the major soft-tissue repair/regeneration QTL regions.

d) Perform two color microarray hybridizations using in-house microarray chips to identify the differentially expressed genes between MRL/MpJ and SJL/J mice or confirm the differentially expressed genes identified by commercial hybridization.

e) To examine if the changes in mRNA expression of candidate genes that are physically localized within the fine mapped soft tissue regeneration QTL regions are associated with the changes in protein expression using SELDI protein chip technology.

The progress for each specific objective is discussed below:

2.   Body

Specific Objectives For The Last Twelve Months Of The Second Funding Period

a) **Specific Objective 1:** To perform QTL mapping using 300 (MRL/MpJ X SJL/J) F2 mice in an attempt to make a linkage map with an even spacing of less than 20 cM between markers.

To accomplish this, we bred MRL/MpJ female with SJL/J male to produce F1 mice. We then produced an F2 population of 500 mice by intercrossing F1 mice and phenotyping each of them at day 25 after ear punch. Genomic DNA was extracted from the liver of each animal in the F2 and parental strain. We tested marker polymorphism between two parental strains (MRL/MpJ and SJL/J) using 410 microsatelite markers from Research Genetics, (Huntsville, Alabama). Informative markers selected were evaluated for spacing between markers across the genome. Additional markers were designed to cover gaps that were larger than 20 cM. The F2 population was genotyped with identified informative markers and additionally designed markers to generate complete genome wide scan. The genotype data was input and organized in a format that is required in order for them to be used in MAPQTL 4.0. We then performed interval mapping using commercial software MapQTL 4.0 and permutation test to determine the significance level of interval mapping.

This objective was accomplished and the results published in 2001 in the Genome Research Journal (Reference -1). We reported these results in the last report for the last six months of the first grand period and first six months of the second grand period.

b) **Specific Objective 2:** To perform commercial microarray hybridization to identify the differentially expressed genes between MRL/MpJ and SJL/J mice.

In order to better understand the molecular basis of soft and hard-tissue regeneration /repair, we made our first generation of a growth factor-enhanced cDNA microarray chip. Our decision to make a growth factor-enhanced microarray chip was guided by the fact that: 1) there is currently no commercially available microarray chip with a similar nature; and 2) it has been well documented that numerous growth factors and their receptors play a key role in tissue regeneration/repair. To accomplish this goal, we extracted RNA from 0.4 mm discs of ear punched tissue (24 hrs after injury) and control tissue and purified poly A RNA using Oligotex kit (QIAGEN). We performed three two-color simultaneous hybridizations: MRL/MpJ control vs. SJL/J control, MRL/MpJ punched vs. SJL/J control and analyzed differential gene expression using an appropriate computational method. Finally, we identified genes that are up-regulated or down-regulated more than two fold after ear punch compared to control and that have more than two fold differential expression between MRL/MpJ and SJL/J mice after ear punch.

After an extensive review of the roles of growth factors/receptors and other important molecules in wound healing, 142 genes were selected for cDNA microarray preparation. Of those, 121 genes were selected from the literature on the basis of their established or suspected roles during wound healing, including 68 growth factor/receptor related genes (56%), sixteen transcription factor/signal transduction molecules, and six metalloproteinases and their natural inhibitors. Twenty-one genes were selected on the basis of their altered expression levels 24 hrs after injury in our previous commercial microarray hybridization, seven of which were ESTs (for a full list of the genes, see Reference -2).

PCR primers were primarily designed to amplify a 3' untranslated region of each gene in order to increase hybridization specificity. The expected PCR sequences were blasted against the gene database to verify that the PCR fragments did not share significant homology with other genes. All PCR products ranging from 300 bp to 1000 bp were evaluated by agarose gel electrophoresis. Reactions with no products, multiple bands, or bands of the incorrect size were considered PCR failures. Ten percent of PCR products were randomly selected for sequence verification. PCR products that passed quality control were purified using a MultiScreen-PCR Filter Plate (Millipore) for printing.

1) Optimum DNA concentration for slide printing is one of the key factors affecting microarray reproducibility. However, its quantitative effect on reproducibility has not been systematically investigated. Currently accepted concentrations for slide printing vary from 0.1 $\mu g/\mu l$ to 0.5 $\mu g/\mu l$. Before printing, we evaluated the effect of seven different DNA concentrations, from 0.01$\mu g/\mu l$ to 1 $\mu g/\mu l$, on signal reproducibility within an experiment and among experiments using Hemoglobin alpha as a target gene. As Figure 1 shows, the signal intensity was increased with the increase of DNA concentration within the range of 0.01$\mu g/\mu l$ to 0.4 $\mu g/\mu l$. When DNA concentration was further increased to 1 $\mu g/\mu l$, the signal intensity was significantly decreased and variation among replicates was increased. Table 1 shows that a DNA concentration of 0.2 $\mu g/\mu l$ was optimal for printing in terms of signal intensity, variation within the experiment, and among experiments under our hybridization conditions.

Based on this study, we diluted the DNA in 3 X SSC at approximately 0.2 $\mu g/\mu l$. The microarrays were printed on the amino-silane coated microscope slides (Corning, NY) using a GMS 417 Arrayer (Genetic MicroSystems). Six replicates of each individual clone were printed on each slide. These replicates will substantially increase the reliability of expression data and make it possible to confidently detect real, but small, changes in expression. Three structural genes were also included as control elements (Mouse group 1 gene for major urinary protein, mouse chromatin structural protein homolog gene, and mouse α-amylase-2 gene). We have made 200 such application-targeted microarray chips for various applications.

2) Temporal analysis of gene expression during wound healing by in-house microarray As an initial attempt, we have used the MRL/MpJ mouse and performed temporal analysis of gene expression during wound healing by using in-house microarray (see Appendix 2-2 for a detailed description).

Fundamental to our understanding of wound-healing biology is knowledge of the signals that trigger relatively sedentary cell lineages at the wound margin to proliferate, become invasive, and then synthesize new matrix in the wound gap. The growth factors are key players in providing the signals to initiate and coordinate this complex process. Topical applications of growth factors to different animal models have demonstrated their ability to accelerate wound healing, providing evidence to support their signaling roles in wound healing. One of the major tasks ahead is to determine the temporal expression profiles and relative concentrations of growth factors and their isoforms at the wound site during healing.

In this study, we used an in-house growth factor/receptor enhanced microarray (68 out of 142 genes are growth-factor related) to determine the temporal gene expression profile of wound healing in the ear-punched tissue of MRL/MpJ-Fas^{lpr} (MRL) mice. Our results: 1) revealed the dynamic change and diverse patterns of gene expression during wound healing; 2) identified three highly-induced genes, at the inflammatory stage, that have not been fully recognized to play a role during wound healing; and 3) showed that well-recognized growth factors/receptors during wound healing are most highly and widely expressed at the repair stage of healing.

To interpret the differential expression data, genes were clustered according to similarity of expression patterns over time points (day 1 represents inflammation stage; days 7 & 14 represent repair stage; and day 28 represents remodeling stage) using the hierarchical clustering approach. Figure 2 shows that differentially expressed genes can be grouped into five major categories (Group A - Group E), each of which has distinctive expression patterns with respect to the stage of healing. For example, genes uniquely up-regulated at the inflammatory stage fall into Group A, while genes up-regulated only at the remodeling stage fall into Group C. Under the defined threshold, 40 genes (28%) were associated with altered mRNA expression at one or more healing stages, 18 of which were growth factor-related (accounting for 26% growth factor-related genes). Of those, 34 (24%) exhibited a ≥1.7-fold increase and six (4%) exhibited a >40% reduction in expression levels. The detailed expression profiles of these genes are presented in Table 2.

One of the most salient findings of this study was that, of the 142 genes studied at all healing stages, three genes (secretory leukoprotease inhibitor, small proline rich protein 2A, calgranulin A) and an EST (accession number of W82549) exhibited the greatest up-regulation at the inflammatory stage, none of which have an established role in wound healing. These three genes had very low basal expression before injury, and the levels of expression were increased 6- to 10-fold 24 hours after injury. Similar levels of induction of these genes were also found in SJL and B6 strains at the inflammatory stage. It is known that the inflammatory stage of wound healing is critical for wound repair, which emphasizes the importance of further studying these genes for their roles in the wound healing process.

c)   **Specific Objective 3:** To build a knowledge-based microarray chip that will include growth factors and other important regulatory genes known to be involved in soft tissue repair/regeneration and the genes that are localized in the major soft tissue repair/regeneration QTL regions.

In order to accomplish this, we have to select relevant growth factors, growth factor receptors and transcription factors within the QTL regions. Primers have been designed for PCR within the 3' untranslated region of the selected genes for the increased hybridization specificity and sensitivity and amplified targeted gene fragments using genomic DNA (PCR) or mRNA (RT-PCR) as template (the average size was about 500 bp). The PCR fragments will be isolated and purified from agarose gel and arrayed in three replicates of each gene fragment on a poly-prep microscope slide using a GMS 417 arrayer.

We have identified 146 genes from chromosome 1 and 164 genes from chromosome 9 using Celera database. The Celera database is a private owned by the APLERA corporation of which we are subscribers. After the selection of genes from the Celera database, we then transferred them to Primer3, a free program from the internet, for primer design. The probes for these genes have been designed using Primer3 and, in addition, PCR amplifications are in the process. Selected genes are as listed in Table 3.

d)   Specific Objective 4: Perform two color microarray hybridizations using in-house microarray chips to identify the differentially expressed genes between MRL/MpJ and SJL/J mice or confirm the differentially expressed genes identified by commercial hybridization.

To accomplish these procedures, we had to prepare high quality mRNA from the ear-punched tissue at three time points corresponding to the inflammatory stage, tissue repair stage, and remodeling stage as well as non-ear-punched control tissue. We make florescence labeled probes (Cye-3 for MRL/MpJ and Cye-5 for SJL/J mice) by reverse transcription and perform multiple two color simultaneous hybridizations. We then scan the hybridization images using Scan Array 4000 (GSI Lumonics) and analyze gene expression profiles using microarray analysis soft ware (BioDiscovery). Lastly, the analysis would reveal the order of appearance or disappearance of those growth factors in response to ear punch or in comparison of MRL/MpJ with SJL/J after ear punch and compare the results from in-house hybridization with commercial source.

For gene expression studies using in house microarray, we have prepared in house microarray slides with more than 6000 genes. We have extracted RNA from good and poor healer strains of mice at three different times during wound healing and performed hybridizations using our in house microarray chips. In order to quantitate gene expression changes reliably, we used 3 replicate RNA samples for each time point. The hybridizations have now been completed and the data analysis is now in progress.

To confirm differentially expressed genes identified by commercial hybridization, we included three genes (secretory leukoprotease inhibitor, small proline rich protein-A and calgranulin A) and an EST (W82549) in our in house microarray chip that contained growth factor genes (please see objective 2). In these studies using in house growth factor gene chip, we confirmed the expression changes in secretory leukoprotease inhibitor, small proline rich protein-A, calgranulin-A and EST W82549 that we

e)   Specific Objective 5. To examine if the changes in mRNA expression of candidate genes that are physically localized within the fine mapped soft tissue regeneration QTL regions are associated with changes in protein expression using SELDI protein chip technology.

Recent studies on gene expression changes using microarray indicate that it is imperative to confirm microarray data using a second method (e.g. real time PCR or Northern blot analysis) with larger number of replicates. Because evaluation of protein expression using SELDI technology is time consuming and expensive, we wanted to make sure that the candidate proteins chosen for this study have been confirmed by a second method.
previously observed during wound healing using commercial microarray.

At this point in time, we have made changes in this objective. Instead of performing SELDI protein chip assays to evaluate changes in protein expression, we

opted to further confirm the genes identified by in-house microarray by use of real time PCR before. The reason was that SELDI protein analysis takes more time and is expensive, so we sought to test only those proteins from genes that have been confirmed further by a second method (real time PCR) that is fast and inexpensive. In place of the SELDI approach, we felt that it was critical to confirm the microarray data with RT PCR. Therefore, we report the development of the RT PCR method and the results (Table 4) instead of the SELDI protein data.

We have optimized the real time PCR using one potential candidate gene from our largest QTL, on chromosome 9. The candidate gene cellular-retinol binding protein1 (CRBP1) has been used to optimize the real time PCR. This gene has different SNPs in the 3' untranslated region between MRL and SJL. The results are shown in Table 4. Before real time PCR we perform a reverse transcriptase (RT) using tRNA from MRL/MpJ (good healer) and SJL/J (poor healer) to amplify cDNA that was then used for real time PCR. We have tested different starting concentrations of tRNA (0.5, 1, 1.5 and 2µg/ µL) and found out that the optimum (gave consistent results) was 1 µg/ µL. The reverse transcription is done using the protocol for Omniscript Enzyme kit from Qiagen (California) using 1 µg/ µLof total RNA. Then 1 to 5µL of this reaction is used to run the real time PCR. To the cDNA we add 2.5µL of 10X Promega buffer, 0.125µL of 10mM dNTPs, 5µL of 5X Reaction Assistant, 0.3µL of 10 pmole forward primer, 0.3µL of 10 pmole reverse primer, 0.1µL Taq polymerase enzyme, 0.5µL of 5X SybrGreen and water to bring solution up to 25µL. The real time PCR procedure is as described by the manufacturer of the DNA Engine Opticon System, PTC-200 DNA Engine Cycler (MJ Research, MA). These conditions will be used to further test the genes identified from in-house microarray data before analysis by the SELDI. We use the cycle number to calculate p values between the control and each time point. The information from p values reflect significant changes in mRNA levels (more or less) our ear punched animals as compared to controls. The results shown in Table 4 are a comparison between the good and poor healer MRL/MpJ and SJL/J respectively.

3. Key Research Accomplishments

- Made 200 growth factor-enhanced microarray chips that contain 142 genes with six replicates.
- Determined the most reproducible DNA concentration for slide printing to be 0.2 µg/µl.
- Examined the temporal transcription profiling of MRL mice during wound healing using in-house microarray chips, which revealed stage-specific genes associated with inflammation, wound repair, or remodeling.
- We have optimized the real time PCR (conditions and tRNA concentration) to further screen genes from the in house microarray.
- Completed the selection of genes to use in building knowledge-based chip with genes from the wound healing/regeneration QTL is complete.

4. Reportable Outcomes

__Full Papers:__

1. Li X, Gu W, Masinde G, Covarrubias M, Mohan S, Baylink DJ (2001) Temporal analysis of gene expression by microarray during wound healing. In press *Wounds*.

2. Masinde G, Li X, Gu W, Heather Davidson, Mohan S and Baylink DJ (2001) Identification of wound healing/regeneration QTLs at multiple time points that explain seventy percent of variance in (MRL/MpJ X SJL/J) F_2 population. Genome Res. 11: 2027-33.

5. Conclusions

We have:
1) Determined the most reproducible DNA concentration for slide printing;
2) Made 200 growth factor-enhanced microarray chips containing 142 genes, each with six replicates; and
3) Performed temporal analysis of gene expression during wound healing in the MRL mouse.
4) Optimized the real time PCR procedure for use in further screening of genes identified from in-house microarray.

Table 1. Effect Of DNA Concentration On Reproducibility Within An Experiment And Among Experiments

DNA Concentration (µg/µl)	Variation Experiment 1 (n=16)	Within	Variation Experiment 2 (n=16)	Within	Variation Experiment 3 (n=16)	Within	Variation Among 3 Experiments (n=3)	
	Mean ±SD	CV%	Mean ±SD	CV%	Mean ±SD	CV%	Mean ±SD	CV%
1	8660±1553	17.9	11920±2062	17.3	7720±2086	27.0	9433±2205	23.4
0.4	32037±4102	12.8	33259±4395	13.2	21649±3313	15.3	28981±6379	22.0
0.3	18483±2804	15.2	19154±1849	9.7	13777±2151	15.6	17138±2930	17.1
0.2	14684±1685	11.5	16027±2044	12.7	13732±2116	14.4	14814±1153	7.8
0.1	5891±963	16.3	5702±1001	17.6	4347±719	16.5	5313±842	15.9
0.05	2094±222	10.6	1838±258	14.0	1267±155	12.2	1733±424	24.5
0.01	1437±85	5.9	1076±107	9.9	731±36	4.9	1081±352	32.7

*Hemoglobin alpha gene was used in this study. Mean value represents average signal intensity from 16 replicate on the slide. One microgram mRNA derived from the liver of different MRL mice was used for Cy5 labeling in three experiments. DNA was dissolved in 50% DMSO and CyScript cDNA labeling kit (Amersham Pharmacia) was used for labeling. The bolded line indicates the optimum DNA concentration for reproducible hybridization signals in consideration of both variation within and among experiments.

Table 2. Gene Expression Profile Of MRL Inbred Strain Of Mice At Three Healing Stages[a].

Gene Group	Gene Name	Accession #	Day 1	Day 7	Day 14	Day 28	Average expression levels of all genes within group
Genes up-regulated during inflammatory stage (Group A)	Secretory leukoprotease inhibitor	AA200339	10.2	1.6	1.7	1.3	
	Calgranulin A	AA230451	7.5	2.0	1.6	1.4	
	EST	W82549	5.8	2.5	2.7	1.7	
	Small proline rich protein 2A	AA497620	4.8	3.3	1.5	1.3	
	Small inducible cytokine A6	AA119293	1.8	1.5	1.5	1.6	
Genes up-regulated during repair stage (Group B)	Estrogen related receptor-α	U85259	1.6	2.6	1.5	1.3	
	TGF-β1	AJ009862	1.4	2.5	1.5	1.1	
	PDGF-β chain	AF162784	1.3	2.3	1.3	1.1	
	Keratinocyte growth factor receptor	M63503	1.5	2.3	1.5	1.4	
	TNF receptor 2	X76401	1.5	2.4	1.7	1.2	
	VEGF-D	D89628	1.4	2.3	1.6	1.2	
	EST	AA064069	1.9	2.1	1.5	1.4	
	TGF β type I receptor	L15436	1.2	2	1.3	1.1	
	Msx-interacting-zinc finger protein 1	AF039567	1.4	1.9	1.4	1.4	
	Lymphoid enhancer binding factor 1	X58636	1.1	2	1.2	1.7	
	Interleukin-8 receptor	D17630	1.3	2.3	1.8	1	
	Fibronectin receptor β chain	X15202	1.1	2	1.2	1.3	
	Ciliary neurotrophic factor receptor α	AF068615	1.3	2.3	1.5	1	
	FGF-8	AF065607	1.1	1.8	1	0.9	
	G-protein coupled receptor kinase 6 D	Y15800	1.3	1.8	1.1	0.8	
	Plasminogen	J04766	1.4	1.8	1.5	0.9	
	Colony stimulating factor-1	X05010	1.3	1.8	1.7	1	
	FGF-1	U67610	1.3	1.7	1.7	1	

Group	Gene	Accession	1	7	14	28
	TNF receptor associated factor 1	L35302	1.3	1.5	1.8	1.2
	Heparin cofactor II	AA253700	1.2	1.5	1.7	1.5
Genes up-regulated during remodeling stage (Group C)	Public domain EST	AA060983	1.3	1.1	1.2	2.5
	Procollagen type III	W89883	0.7	0.4	0.6	2.2
	Metallothionein 2	AA203775	1	1.5	1.6	2.2
	Membrane type 3 metalloprotinase	AB021228	1.1	1.6	1	1.9
	Urokinase-type plasminogen activator	M17922	1	1.6	1	1.8
	IGFBP-1	X67493	1.2	1	1.3	1.8
	BMP type II receptor	U78048	0.9	0.9	1.3	1.7
Genes up-regulated during inflammatory and remodeling stages (Group D)	IGFBP-2	X81580	2	1	1.5	2.1
	Tenascin	D90343	2.3	1.6	1.4	1.8
Genes down-regulated after wounding (Group E)	Tissue inhibitor of metalloproteinase-2	X62622	0.3	0.3	0.3	0.4
	BMP8b	U39545	0.5	0.6	0.6	0.5
	Hemoglobin α adult chain	AA109900	0.9	0.2	0.1	0.3
	Tenascin-X	X73959	0.6	0.5	0.5	0.5
	EST	AA190040	0.6	0.5	0.4	1.1
	Selenoprotein P	AA276440	0.6	0.3	0.3	1.5
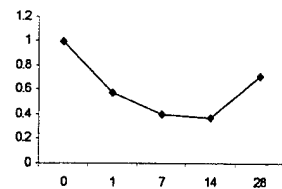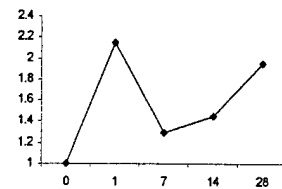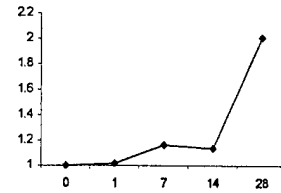
[a]Day 1 represents inflammatory stage; Days 7 and 14 represent repair stages; Day 28 represents remodeling stage. Genes listed here are either up-regulated (≥ 1.7 fold) or down-regulated (≤ 0.6 fold) at least at one of the healing stages (bolded). Fold changes in the Table are all relative to the control intensity (Day 0). X axes represent days after ear punch and Y axes represent fold changes.

Table 3: Some of the genes selected from chromosome 1 and 9 to make knowledge based chip for genes within the wound healing/regeneration QTLs.

High affinity interleukin-8 receptor A	Cell adhesion molecule-related
High affinity interleukin-8 receptor B	**Coiled-coil Protein**
ARP2/3 complex 34kd subunit-related	GAG Polyprotein
Angio-associated migratory cell protein	Mitotic Chekpoin Protein BUB3
Lifeguard-related	T-Box protein
Hydroxyacylglutathione hydrolase-related	Line-1 Reverse Transcriptase-related
Natural resistance-associated macrophage protein SLC11A1,2-related	High Mobility Group Protein HMG1-Related
Nuclear LIM interactor-interacting factor	Mitochondrial Carrier Protein
Villin	5'-Nucleotidase
Ubiquitin carboxyl-terminal hydrolase required for cell differentiation homolog 1(red 1)	Putative Protein (NS1- associated protein 1)
Phospholipase C delta-4	Krueppel-related C2H2 Type Zinc Finger protein
gb def: zinc finger protein 142	Testis-Specific ring finger protein
AAA-family ATPase	Cytochrome P450 A1, aromatic compound inducible
Serine/threonine kinase fused	
Cytochrome p450 27, mitochondrial	Ply(A)-bindind protein testis-specific (PABPT)
5'-AMP-activated protein kinase, gamma-1 subunit	
WNT-6 protein	Cop-coated vesicle membrane protein p24 related
WNT-10 protein	Ankyrin repeat-containing protein
Cyclin-dependent kinase 5 activator 2	VAV proto-oncogene related (RAS protein-specific guanine nucleotide releasing factor 1)
Retroviral integration site protein FLI-1-related	
beta crystallin A2	Cathepsin H-related
Hedgehog	Trascription factor MRG-related
gb def:(u25739) yspl-1 form 1	Adam-Ts 7
ATP-binding cassette transporter ABCB 7-related	Rab GTPase Activating Protein-Related
	60S RIBOSOMAL PROTEIN L35A
Beta -galactosidase	REVERSE TRANSCRIPTASE RELATED
myristilated and palmitylated serine-threonine kinase-related	REVERSE TRANSCRIPTASE RELATED
	gd def: (ab012223) orf2 (canis familiaris)
tubulin alpha chain	60S RIBOSOMAL PROTEIN L9
DNAJ-related	ribosomal protein L37
Protein-tyrosine phosphatase x-related	RETROVIRUS RELATED POL POLYPROTEIN
Aspartyl aminopeptidase	
gb def: striated muscle-specific serine/threonine protein kinase	TUBULIN ALPHA CHAIN
	ZIC 1
Mannose-1 phosphate guanyltransferase	zIC-RELATED
Amiloride-sensitive brain sodium channel BNAC	REVERSE TRANSCRIPTASE RELATED
	Line-1 Reverse Transcriptase-related
gb def: (ab014557) kiaa0657 protein	REVERSE TRANSCRIPTASE RELATED

Inhibin alpha chain	REVERSE TRANSCRIPTASE RELATED
Protein phosphate regulatory subunit-related	procollagen lysine, 2-oxaglutarate 5-dioxygenase
anion exchange protein 3/slc4a3-related	Line-1 Reverse Transcriptase-related
gb def: kruppel-associated box protein	integrin alpha-6
60 s ribosomal protein L7A	Glyceraldehyde 3-phosphate dehydrogenase
Reverse transcriptase-related	
Reverse transcriptase-related	REVERSE TRANSCRIPTASE RELATED
60s ribosomal protein L17	60s ribosomal protein L13A
Ephrin receptor	Sodium/hydrogen exchanger-related
Reverse transcriptase-related	sodium/hydrogen exchanger-related
Paired box protein PAX-3	N-acetylglucosamine-6-o-sulfotransferase
Phenylalanyl-TRNA synthetase	Ribonucleoprotein
Long-chain-fatty-acid--CoA ligase	Procollagen C-proteinase enhancer protein
Glia-derived nexin	Transient receptor potential channel 1
ADP, ATP carrier protein	I-plastin
Cullin homolog 3	DNA repair protein RAD 3-related
40s ribosomal protein SA-related	
Insulin receptor substrate-1	glyceral kinase
Collagen alpha4 (IV) chain	Sodium/potassium dependent ATPase beta-3 subunit
Collagen alpha3 (IV) chain	
30s ribosomal protein S14-related	ring finger protein
REVERSE TRANSCRIPTASE RELATED	GTPase activating protein RAS
	Krueppel type zinc finger protein
	40s ribosomal protein S2
procollagen lysine, 2-oxaglutarate 5-dioxygenase	acid phosphatase related
	peptidyl-prolylcis-trans isomerase related
Line-1 Reverse Transcriptase-related	histone H3
integrin alpha-6	Mitochondrial Carrier Protein
glyceraldehyde 3-phosphate dehydrogenase	Nicotinamide mononucleotide adenylyl transferase-related
REVERSE TRANSCRIPTASE RELATED	
60s ribosomal protein L13A	40S ribosomal protein S7
Sodium/hydrogen exchanger-related	Retinol-binding protein I-related
Sodium/hydrogen exchanger-related	Retinol-binding protein II
N-acetylglucosamine-6-o-sulfotransferase	Coatomer beta subunit
Ribonucleoprotein	Pol polyprotein
Procollagen C-proteinase enhancer protein	Thiamine transporter SLC19A2
Transient receptor potential channel 1	Small inducible cytokine A20
I-plastin	Eukaryotic translation initiation factor 2 alpha subunit
DNA repair protein RAD 3-related	
Glyceral kinase	wd40 repeat protein
Sodium/potassium dependent ATPase beta-3 subunit	Reverse transcriptase-related
	Fibropellin
ring finger protein	Epidermal growth factor-related protein
GTPase activating protein RAS	GB def: thyroid hormone receptor interactor 12; thyroid Receptor interacting
Krueppel type zinc finger protein	

40s ribosomal protein S2 Acid phosphatase related Peptidyl-prolylcis-trans isomerase related histone H3 Mitochondrial Carrier Protein 60s ribosomal protein L7A Pyruvate kinase Heterogeneous nuclear ribonucleoproteins A1 related S100 calcium-binding protein C Zinc finger transcription factor Cadherin	protein 12 Monocarboxylate transporter 60s ribosomal protein L7A Pyruvate kinase Heterogeneous nuclear ribonucleoproteins A1 related S100 calcium-binding protein C Zinc finger transcription factor Cadherin

Table 4: The results of real time PCR using a potential candidate gene cellular retinal binding protein 1 (CRBP1) showing the strain, cycle number, mean, standard deviation, number of replicates, p value, and whether up- or down regulated in MRL (good healer) and SJL (poor healer).

| Mouse strain	Time Point	Cycles	Mean	SD	N	p Value	mRNA change vs. control
MRL	Control	28.7 28.6 29.0	28.9	0.19	3	MRL	Control
MRL	4 HR	26.0 26.3 26.6	26.4	0.28	3	p<0.0002	UP
MRL	D1	26.3 26.6 26.7	26.4	0.28	3	p<0.0002	UP
MRL	D7	26.4 26.6 25.9	26.4	0.40	3	p<0.0007	UP
MRL	D14	27.3 27.4 27.8	27.5	0.29	3	p<0.0034	UP
MRL	D28	28.3 28.1 28.3	28.3	0.11	3	p<0.02	Same
SJL	Control	25.2 25.2 24.5	25.1	0.41	3	SJL	Control
SJL	4 HR	24.5 24.1 24.0	24.1	0.26	3	p<0.05	Same
SJL	D1	25.0 24.7 25.0	25.0	0.17	3	p<0.84	Same
SJL	D7	27.6 27.8 27.5	27.7	0.16	3	p<0.0005	Down
SJL	D14	27.5 27.9 27.2	27.6	0.35	3	p<0.001	Down
SJL	D28	26.9 26.1 25.6	26.3	0.66	3	p<0.06	Same
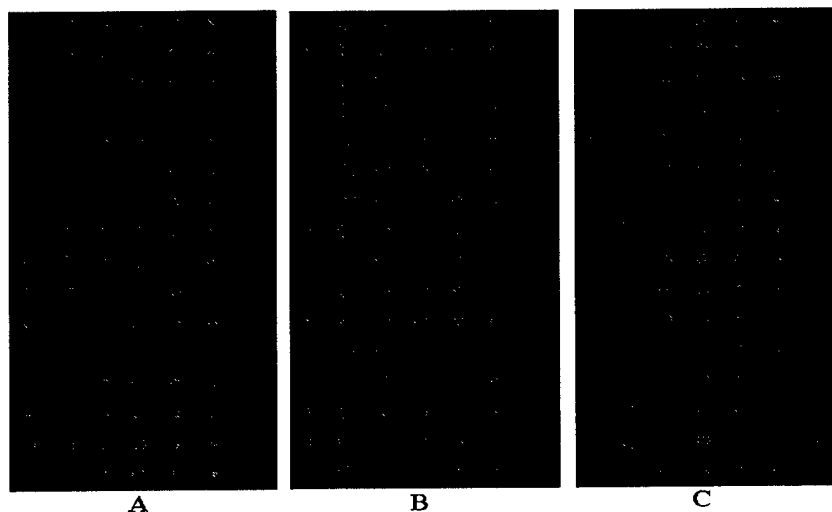
Fig 1. The effect of DNA concentration on reproducibility of microarray hybridization. The microarray images of Hemoglobin alpha gene are shown for three independent hybridizations (A, B, and C) using mRNA isolated from the liver of different MRL mice. The columns represent 16 replicates and rows represent 7 DNA concentrations for printing (from left to right: 1μg/μl, 0.4μg/μl, 0.3μg/μl, 0.2μg/μl, 0.1μg/μl, 0.05μg/μl, and 0.01μg/μl). The quantitative analysis of the DNA concentration-dependent reproducibility is shown in Table 1. For the detailed hybridization procedures, see footnotes in Table 3 and previous publication (1).
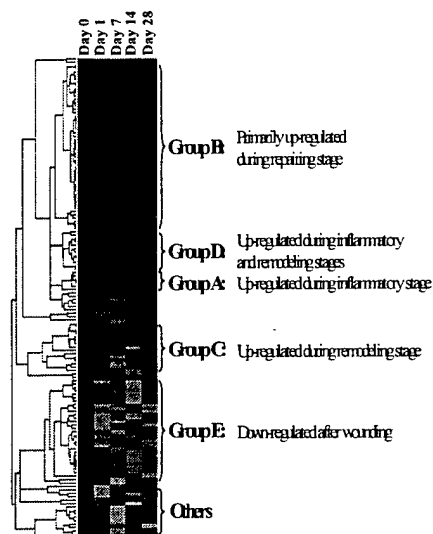

Fig 2. Cluster analysis of gene expression profiles. The image shows the different classes of gene expression over four time points. One hundred and forty two genes were clustered hierarchically into groups on the basis of the similarity of their expression profiles and magnitudes by the procedure of Eisen et al. The expression pattern of each gene is displayed here as a horizontal strip. For each gene, the ratio of mRNA levels in the ear-punched tissue at the indicated time point to its level in the non-ear-punched control tissue is presented by a color. Red indicates that the gene is up-regulated in comparison to the control whereas green indicates the opposite. Sets of genes that clustered together and were either repressed or induced at different healing stages are indicated as group A − F.

C. Technical Objective 3: To apply the N-ethyl-N-nitrosourea (ENU) mutagenesis to identify new genes that regulate soft- and hard-tissue regeneration in C3H strain of mice.

1. Introduction

The goal of this Technical Objective is to identify and characterize novel genes or to elucidate function for known genes that play a key role in the metabolism of bone and soft tissue using the ENU mutagenesis technique.

During the last 12-months of the second funding period, we have proposed the following specific objectives.

a) To generate ENU treated C3H male founder by injecting three weekly doses of 100 mg/kg solution intraperitoneally.
b) To design a mating scheme to generate 50 F1 mice per week by crossing the ENU mutagenized C3H male mouse to its wild type female partner.
c) To use previously optimized phenotype screening procedures to screen: 1) body weight; 2) soft-tissue regeneration; 3) muscle size; 4) bone density; 5) bone formation markers; 6) bone resorption markers; and 7) a marker of lipid metabolism.
d) To screen 1300 F1 C3H mice following the procedures described above.
e) To confirm mutant phenotype by: a) repeating the measurement of concerned phenotype; and b) back-crossing to C3H wild type female.
f) To preserve sperm of mutant mice by the cryopreservation technology.
g) To identify lines of mice with chromosomal deletions for studies on recessive mutation.

2. Body

Our specific objectives during this reporting period were to generate and screen C3H/HeJ (C3H) mice for skeletal phenotypes caused by dominant mutations. However, during this reporting period, we have performed phenotypic screening of dominant as well as recessive mutations. In addition, we have included a low bone density C57BL/6J (B6) mice strain (in addition to C3H mice) in our dominant screening. The rationales for these changes are mentioned below.

i) Multiple genes regulate phenotypes such as bone density and soft tissue regeneration. Some genes act in a dominant manner, in that disruption of a single copy of the gene causes phenotypic changes, while others act in a recessive manner, in that disruption of both copies of the gene are needed to produce the abnormal phenotypic changes. Complex phenotypes such as bone density and soft tissue regeneration are likely to be regulated by both dominant and recessive sets of genes. Therefore, we have generated and screened both dominant and recessive mutations in C3H mice.

ii) Our main aim of using ENU mutagenesis in the mouse model is to identify genes that regulate the musculoskeletal phenotype in mice. We have earlier identified that C3H mice have the highest bone mineral density (BMD) and B6 mice have the lowest BMD among 13 inbred strains. Our experience with

ENU mutagenesis in C3H mice indicates that most of the mutations that we have observed so far are loss-of-function mutations. Based on this observation it can be assumed that use of a strain with low BMD mice is a good candidate for identifying mutations that may result in an increase in bone density. Therefore, we have included B6 mice in our dominant screening. The breeding characteristics of B6 mice are similar to C3H mice and the B6 mouse can tolerate ENU well with a high fertility rate after an initial recovery period. Therefore, use of B6 mice will not affect the number of mice screened from each ENU injected male.

Specific Objectives For The Last Twelve Months Of The Second Funding Period

a)   Specific objective 1: To generate ENU treated C3H male founder by injecting three weekly doses of 85 mg/kg solution intraperitoneally.

Earlier, we reported that the optimum dose for C3H was 3x100 mg/kg. Therefore, in the current reporting period, we have injected two batches of 8-10 week old 20 C3H/HeJ male mice with 3x100 mg/kg of ENU. Both these batches of ENU injected male were used for generating F1 progeny. In addition, we injected two batches of 20 6-8 week old B6 males with 100 mg/kg of ENU, which was used to generate B6 F1 progeny.

b)   Specific objective 2: To design a mating scheme to generate 50 F1 mice per week by crossing the ENU mutagenized C3H male mouse to its wild type female partner.

All C3H and B6 male mice (four batches of 20 mice each) were injected with 3X100 mg/kg ENU at 10-12 week intervals. This gap allowed us a continuous supply of ENU mutagenized C3H or B6 males for breeding with C3H or B6 wild type females. By breeding each ENU injected male with two wild type females, we insured that about 50 dominant or recessive progeny were screened every week. Data on the sterile period, percent of mice that recovered fertility, and litter size is described in **Table 1**. The B6 mice recovered early (15-20 weeks) and produced a higher number of pups from ENU injected males, as compared to ENU injected C3H male mice.

The generation and screenings of B6 mice were performed as described for F1 C3H mice in our earlier report. To generate C3H F3 mice for recessive screen, we bred about 15 randomly selected F1 males with 75 wild type C3H females (**Figure 1**). Approximately 450 F2 male and female pups were generated from these crosses. We bred approximately 225 female F2 pups with 15 F1 male (founder male). So far, we have screened 545 F3 progeny generated from F2 (female) X F1 male for recessive mutations affecting: a) body weight; b) soft-tissue regeneration; c) muscle size; d) bone density; e) bone formation markers; f) bone resorption marker; and g) growth markers.

c)   Specific objective 3: To use previously optimized phenotype screening procedures to screen: a) body weight; b) soft-tissue regeneration; c) muscle size; d) bone density; e) bone formation markers; f) bone resorption markers; and g) a marker of lipid metabolism.

In the previous report, we reported optimization of phenotype screening procedures to screen: a) body weight; b) soft-tissue regeneration; c) muscle size; d) bone density; e) bone formation markers; f) bone resorption markers; and g) a marker of lipid

metabolism. We have performed two additional optimizations for quantitative musculoskeletal phenotype screening. We now screen mutagenized mice at 10-weeks of age as compared to 6-weeks as described in our previous report. This was done to minimize the false positives resulting from the higher variation seen in 6-week old mice as compared to 10-week old mice. The second optimization was performed to distinguish mutations that affect bone size from those that affect growth. This was done because size sensitive parameters are influenced by body size, which means a small mouse will have a lower BMD (by DEXA measurements), BMC, or bone size than healthy, age-matched non-mutagenized control mice, even if their bones (smaller) are otherwise completely normal. To overcome this technical problem, we have developed an empirical formula to adjust size phenotypes with body weight for screening bone size mutants.

Further details of these optimizations are described below.

Optimization of screening age of mutagenized F1 or F3 progeny: The C3H mice attain peak bone density when they reach 16-weeks of age and, thereafter, BMD declines with age. For a cost efficient ENU screening, one would like to identify the skeletal phenotypes in an early age group. However, the most reliable results on BMD measurements were obtained at 16-weeks age, when these mice attain peak-bone density. This is illustrated in **Figure 2**, which shows CVs of three selected parameters (BMD, BMC, and Bone Area) obtained by DEXA in 6-week, 10-week, and 16-week old mice. The population CVs consistently decreased from the high (in 6-week old mice) to lowest (in 16-week old mice). A high variance, as seen in 6-week old mice, would lead to classification error and a high rate of false positive or negative outliers. Therefore, we selected the 10-week time point for screening; this minimizes the housing cost with a minimal loss of precision as compared to the 16-week mice. Since outlier mutants were identified by comparison with age and sex matched normal ranges, we obtained additional normal range data from 10-week and 16-week old male and female mice (**Tables 2 & 3**).

Outlier Assessment of Phenotype Traits Affected by Size: Size parameters, such as BMC, bone area, femur BMD, and endosteal and periosteal circumference, are size-dependent and show a strong correlation with body weight (**Table 4**). Hence, it is necessary to normalize the bone mass and bone size data in F1 and F3 progeny with body weight. To derive the body-weight-adjusted bone size traits data, we regressed each of the size traits with body weight using male (n=60) and female (n=60) non-mutagenized control mice that are 10-weeks and 16-weeks old. We analysed the correlation with regression analysis and developed an estimating equation to normalize size traits in F1 and F3 progeny. For example, the following formula was used for adjusting size sensitive traits in female 10-week C3H mice determined by PXIXImus: [Adjusted Size Trait = Non-Adjusted Size Trait/(Slope × Body Weight + Intercept) where Intercept and Slope are from regression analysis of this Size Trait in 10-week normal female population (n=60)]. The observed weight-adjusted values for size parameters showed statistically non-significant and negligible correlations with body weight (**Table 4**). This manipulation allowed us to compare all parameters on one scale including male and female data.

d)   Specific Objective 4: To screen 1300 F1 C3H mice following the procedures described above.

Phenotype screens were carried out under one episode of anesthesia at 10-weeks of age to identify abnormality in growth, bone density, tissue regeneration capacity, and bone metabolism. An abnormality is recognized if a phenotype differs by three standard deviations (±3SD) as compared to baseline values obtained earlier using age and sex matched non-mutagenized C3H mice. Measurements that are found to be abnormal are repeated at 16-weeks to confirm the phenotype. For this purpose, we have obtained additional baseline values for age and sex matched C3H mice for 16-weeks of age **(Tables 3 & 4)**.

We have screened a total of 1865 mice during this reporting period. These include 228 C3H F1 mice for dominant screening, 545 C3H F3 mice for recessive screening, 452 B6 F1 mice for dominant screening, and 640 mice in Inheritance Testing. In addition, we have screened additional 200 mice to generate normal data for 10-week and 16-week old C3H and B6 mice. This brings the total number of mice screened during this reporting period to 2065. We describe each phenodeviants separately in each of these screening categories. Details of Inheritance Testing mice are described in Specific Objective 5.

C3H Dominant and Recessive Screen

Visible phenotypes: We have reported several visible abnormalities in our previous report. In this report, we describe a new mutant with a visible, as well as quantitative, abnormality. The outlier mouse was identified in recessive screening and the phenotype has yet to be fully characterized **(Figure 3A** shows the mutant mouse along with a normal littermate). The affected mice appear weak, have low body weight, splayed gait, and show fur with a greasy appearance early in development (birth to 5-6 weeks of age). The affected adults have normal fur but with increased yellow pigmentation at skin surface and low BMD. We have generated four second-generation affected progeny and all of them show reduced bone density parameters. The total body BMD was 8% lower (p<0.0001) in affected progeny **(Figure 3B & 3C)**. In addition, the body weight adjusted BMC and bone area were 15-20% lower (p<0.0001).

Quantitative Phenotypes: We have screened 773 mice in dominant and recessive screenings. Representative phenotypic data on mutagenized progeny is shown in **Figure 4**, including both body weight adjusted and non-adjusted BMD and BMC in about 200 male and 200 female F3 progeny. Mice that were outside the adjusted, as well as non-adjusted, reference range were retested at 16-weeks. Those confirmed as extreme scoring outliers were subjected to inheritance testing. All phenodeviants identified in the dominant and recessive screen in this reporting period are shown in **Table 5**, including those that were not yet confirmed in inheritance test cross.

B6 Dominant Screen
We have screened 452 F1 B6 progeny **(Table 6)** for all phenotypes listed in Specific Objective 4. We observed 9 phenodeviants in our primary screening performed at 10-

weeks and confirmed five quantitative phenodeviants in 16-week repeat testing; these phenodeviants are listed in **Table 7**, which include those that were not confirmed in inheritance test cross.

e) **Specific Objective 5:** To confirm mutant phenotype by: a) repeating the measurement of concerned phenotype; and b) back-crossing to C3H wild type female.

Our screening strategy involves repeat testing at 16-weeks for all phenodeviants identified in the 10-week screening. In repeat testing, we used peripheral quantitative computed tomography (pQCT), in addition to PIXI, to measure bone density at 10- and 16-weeks of age. Those phenotypes that are confirmed after repeat testing are subjected to inheritance-test (IT) or backcross with wild type mice. We observed that several of the phenodeviants identified in the 10-week screen had lower than 3SD units difference when retested at 16-weeks (**Table 6**). Because of the significant efforts involved in progeny testing, we have focused on those phenodeviants that had the highest differences in phenotypes, which is independent of body weight (and body size).

Each phenodeviant is mated with 1-2 normal wild type male or female mice. Once the mating is successful, pregnant mice are separated and placed separately to give birth to B2 littermates. If the F1 affected mouse is a female, it is reintroduced for mating to produce 3-5 litters totaling about 20-25 F2 pups. If the affected mouse is male, 3-5 female mice are mated simultaneously.

The IT F2 offspring were screened at 10-weeks and 16-weekss of age. A mutation is considered inheritable if the phenotype is recovered in both the B2 and B3 progeny.

In the current reporting period, we introduced 17 mice (including both C3H & B6) into inheritance testing by mating affected male and female with wild type C3H or B6 mice. All outlier mice that are under inheritance testing are listed in Tables-6 & 7. We have screened at least 20 progeny from these matings to assess inheritance of phenotypes. We have recovered four dominant C3H and one B6 phenodeviants with about 48-53% of litter mates affected. In one recessive mutation, about 26% of IT progeny were affected. In both cases, the ratio of affected and non-affected litter mates was close to the expected ration for dominant (50% affected) or recessive mutation (25% affected). Characteristics of five mutants confirmed in the inheritance testing are discussed separately in the preceding section.

<u>Inheritance Test Results from C3H Dominant and Recessive Mutants</u>

Below, we present data on three different musculoskeletal phenodeviants that were confirmed in the progeny test. The fourth phenodeviant confirmed in inheritance crosses had 20% decreased body weight as compared to littermates.

i) <u>Phenodeviant with decreased bone size:</u> Data from 16-week old progeny from phenodeviant 5.37.5 is shown in Figure – 5. The affected progeny was identified as <3SD units lower total BMC compared to normal mean. The first and second-generation progeny shows an approximate 0.9:1 [affected (n=31): non-affected (n=36)] Mendelian ratio. The average body weight adjusted total body BMC was decreased by 14%

(p<0.00001), whereas BMC at the mid shaft of tibia was 15% decreased as compared to litter mates. The adjusted total body bone area was lower by 14% (p<0.00001), mean periosteal circumference was 9% lower (p<0.00001), and average endosteal circumference was 15% lower (p<0.00001) (Figure 4), as compared to non-affected progeny. The total BMD (-2%, p=NS) and cortical BMD were not significantly decreased in affected or non-affected progeny. The biochemical markers were not significantly different between affected and non-affected progeny. Summary of all data indicates that mutation causes reduced bone size.

ii) Decreased tibial bone size that exceeds the decrease in total bone size: Figure – 6 shows offspring from outlier mouse 6.5.5, which segregated as 0.9:1 [affected (n=11):non-affected (n=12)] in first-generation progeny. The affected mice were identified because of low bone area (<3SD) at mid-shaft of tibia. The affected progeny had a mean decrease of 12% in bone area at mid-shaft of the tibia. The total body bone area was, however, only 6% (p<0.05) lower in affected progeny. In addition, we observed about 5% lower periosteal circumference (p<0.01), and about 15% lower endosteal circumference, in affected mice. In summary, the affected offspring showed significantly lower bone size parameters at the tibia and a much smaller decrease in total body bone area. There was no significant difference in BMD in affected and non-affected litter mates.

iii) Decrease in bone density: Figure – 7 shows BMD data from an outlier (5.27.7) identified in our recessive screen. Data represents F3 progeny from six litters, which were generated from crosses between heterozygote F2 female and male mice. The average body weight adjusted data from affected progeny showed 8% lower total body BMD, 9% lower femur BMD, and 18% low total body BMC, as compared to un-affected littermates (Figure – 7). The total BMD and total BMC measured by pQCT at the mid-diaphysis of the tibia were 3% lower (p<0.05) as compared to un-affected littermates.

Biochemical marker phenotypes: Earlier, we reported on two F1 mice with abnormal biochemical marker levels. We have progeny tested both these phenodeviants.

1) Increased skeletal alkaline phosphatase levels – An F1 female mouse was identified with about 70% higher skeletal alkaline phosphate activity in blood as compared to age and sex matched normal mice. In addition to possessing high skeletal alkaline phosphatase activity, this F1 mouse was hyperactive and has shown constant circling behavior. While this mouse was bred for inheritance testing, it has shown difficulties in nursing the pups. Our attempts to use a foster mother (FVB mice) to rescue the litters have not been successful.

2) Decreased C-telopeptide (type-I collagen) levels - The C-telopeptide is a marker of bone degradation and low levels of this marker could be associated with a low rate of bone resorption. Progeny testing of this mouse is still continuing.

Inheritance Test Results from B6 Dominant Mutant

We have tested five outlier in inheritance testing and confirmed one outlier as an inheritable mutant. Details of phenotypes in the confirmed phenodeviant are shown in

Figure 8. Data from 16-week old progeny from outlier 9.1.7 shows that body weight adjusted total body bone area was 16% lower (p<0.0001) in affected (n=17) progeny as compared with non-affected littermates (n=23). The mean BMC was 15% lower in affected progeny. In addition, the affected mice had 6% (p<0.05) lower periosteal circumference at the mid shaft of the tibia. These data indicate that mutation is affecting bone size at multiple skeletal sites.

f)   Specific Objective 6: To preserve sperm of mutant mice by the cryopreservation technology.

To initiate cryopreservation of mouse germplasm, we have established a small cryopreservation lab. We acquired all equipment needed for sperm cryopreservation and obtained approval of animal protocol (ACORP) to allow surgical procedures, handling of embryos, sperm, and ovaries in several strains of mice.

We have trained technicians in the techniques of survival and non-survival surgical procedures to remove epididymides and vas deferentia from male mice. We are currently training technicians in freezing sperms. Our aim is to: 1) cryopreserve and revive sperm collected from normal mice; 2) perform *in-vitro* fertilization with cryopreserved sperm and fresh oocytes collected from super-ovulating females to test the successful accomplishment of preservation techniques; 3) implant embryos in pseudopregnant females and generate live pups; and 4) maintain long-term storage of embryos, ovaries, and sperms in liquid nitrogen. We propose to perform cryopreservation of sperms from only those phenodeviants that both demonstrate key phenotypes and are confirmed via inheritance testing.

g)   Specific Objective 7: To identify lines of mice with chromosomal deletions for studies on recessive mutation.

The strategy for region (deletion) specific mutagenesis involves a two-generation breeding scheme. In the first step, male mice injected with ENU are crossed with wild type females. The resulting progeny are then crossed with mice that bear a known chromosomal deletion. The offspring that inherit the deletion from one parent and an altered/mutated gene from the other parent will display a mutant phenotype. The most critical requirement for the region-specific mutagenesis is mice (deletion lines) that bear a known chromosomal deletion and, in our case, deletion in the region of chromosomes that harbors QTLs affecting skeletal phenotypes. To find out which chromosomal deletion will be useful to us in region-specific mutagenesis, we reviewed all published major QTLs regions described in mouse progenitor strains that affect skeletal phenotypes and soft-tissue regeneration. These QTL regions are shown in Table 8 and are used as a guideline for identifying deletion lines that may be useful for us to initiate region-specific mutagenesis.

We found that mice that have chromosomal deletion (as shown in Table 8) are not available. However, ES cell clones that contain deletions or vectors integrated throughout the genome that can be used for subsequent generation of deletion mice are listed in a bank (DelBank, Merk Genome Research Institute, West Point, PA). Currently, there are about 110 mapped DelBank clones. The DELBank clones are made available to

the general academic/scientific community, free-of-charge, and can be used to generate deletion lines. We have identified several ES lines (shown in Table 8) that are in the region of our interest (QTLs that harbor skeletal phenotypes). From this list shown in Table – 7, deletion mice could be only derived for one or two selected ES clones because of the large expense involved in generating the transgenic mouse.

3.   Key research accomplishments

- We have screened 1865 F1 & F3 offspring for bone and growth related abnormalities.
- We have initiated recessive screening in addition to ongoing dominant screening in C3H/HeJ mice.
- We initiated a dominant screening in a low bone density B6 mouse strain.
- We have identified 26 phenodeviants in F1 & F3 C3H mice. We identified 9 phenodeviants in F1 B6 mice.
- We have confirmed 12 C3H phenodeviants and 5 B6 phenodeviants in repeat testing.
- We progeny tested 12 C3H and 5 B6 phenodeviants.
- We have confirmed four C3H phenodeviants and one B6 phenodeviant in inheritance testing.
- We have initiated crosses between mutant strain and a mapping strain for genotyping mutation.

4.   Reportable outcomes

Abstracts

Srivastava A K, Mohan S, Wergedal J E & Baylink DJ (2002) A Genome-wide Screening of N-Ethyl-N-nitrosourea Mutagenized Mice for Musculoskeletal Phenotypes. J Bone & Miner Res:17(1);S176 / (Oral presentation at 24th Annual Meeting of American Society for Bone and Mineral Research, 21-24 September 2002)

Full papers

Srivastava A K, Mohan S, Wergedal J E & Baylink DJ. A Genome-wide Screening of N-Ethyl-N-nitrosourea Mutagenized Mice for Musculoskeletal Phenotypes. Manuscript Communicated, 2002.

5.   Conclusions

We have injected two batches of C3H/HeJ and C57BL/6J males with an ENU dose of 3 X 100 mg/kg to generate ENU founder male. We have established the sterility and fertility period at the dose of 3 X 100 mg/kg. We have established a breeding scheme to generate about 50 F1 or F3 progeny per week. Therefore, we have achieved the first three objectives of the study.

We have further optimized screening of quantitative phenotypes (especially size traits) and we have screened 1865 F1, F3, and IT mice during this reporting period of the project. In addition, we have screened 200 mice to generate normative data. Thus, the

total number of mice screened was 2065, and, therefore, we have achieved our third and fourth objectives of the study.

We have tested the inheritability of 16 phenodeviants and confirmed 5 phenodeviants as inheritable mutations. Therefore, we have achieved the fifth objective of repeat testing and confirming the inheritance of observed mutations.

We have established a cryopreservation lab and completed training in cryopreservation of mouse sperm. We were holding the cryopreservation until the phenodeviants are confirmed in the inheritance test, which we have achieved now and have initiated the sperm freezing process. Thus, we have made significant progress on the sixth objective of this study period.

Finally, we have compiled a list of major QTL regions that affect skeletal phenotypes and soft tissue regeneration in different progenitor mouse strains. We have looked into the availability of deletion mouse lines in the region of our interest and found that, at present, such lines are not available. However, ES cell lines that contain deletions in our region of interest are available and could be used to generate transgenic mice with known chromosomal deletions. Thus, we have achieved the final objective of this study period.

Table 1. Response of C3H/HeJ and C57BL/6J mouse strains to 3 X 100 mg/kg dosage of ENU.

	C3H/HeJ (C3H)	C57BL/6J (B6)
Percentage of males died before regaining fertility	20-35%	10%
Return to fertility (Weeks)	20-22	15-20
Percent males sterile	50%	40%
Average Litter size	4.1	6.6

Table 2. Reference range values of bone density and other parameters determined by Dual Energy X-ray Absorptiometery (DEXA) on 6-, 10-, and 16-week old non-mutagenized C3H/HeJ mice

Phenotype	Sex	6-Week Old Mice		10-Week Old Mice		16-Week Old Mice	
		Mean±SD (n=37)	Population Variance (CV)	Mean±SD (n=38-46)	Population Variance (CV)	Mean (n=40)	Population Variance (CV)
Weight (g)	F	17.2±1.6*	9.5	19.7±1.4*	7.2	21.8±1.6*	7.3
	M	21.2±1.7	7.8	24.8±1.5	6.0	28.1±1.5	5.4
Total Body BMD (g/cm^2)	F	0.0391±0.0023	5.8	0.0476±0.0018	3.8	0.0547±0.0018	3.4
	M	0.0411±0.0020	4.9	0.0481±0.0018	3.4	0.0545±0.0018	3.4
Total Body BMC (g)	F	0.298±0.0296*	9.9	0.454±0.0342*	7.5	0.539±0.036*	6.7
	M	0.338±0.030	9.0	0.483±0.030	6.3	0.582±0.038	6.5
Total Body Bone Area (cm^2)	F	7.6±0.5*	6.9	9.54±0.45*	4.7	9.9±0.5*	4.6
	M	8.2±0.6	7.7	10.0±0.40	4.6	10.7±0.52	4.9
Total Body Muscle mass (g)	F	7.4±0.71*	9.7	8.16±1.16*	13.9	10.2±1.5*	14.6
	M	10.2±1.1	9.8	12.8±1.20	9.7	15.7±1.34	8.6
Femoral BMD/CM^2	F	0.0505±0.032*	6.3	0.0678±0.0026*	3.9	0.080±0.003*	4.3
	M	0.0596±0.036	6.1	0.0754±0.004	5.4	0.085±0.006	6.7
Total Body BMD adjusted with Bone Area	F	0.0425±0.025	6.0	0.0462±0.0015	3.2	0.0547±0.0018	3.4
	M	0.0431±0.027	6.3	0.0455±0.0015	3.3	0.0545±0.0018	3.4
Total Body BMC adjusted with Bone Area	F	0.324±0.024*	7.4	0.440±0.024*	5.6	0.515±0.025*	5.6
	M	0.353±0.022	6.1	0.457±0.021	4.6	0.534±0.024	4.6

*Male significantly different from female.

Table 3. Reference range values of bone density and other parameters determined at mid-diaphysis of tibia by peripheral quantitative computed tomography (pQCT) on 6-, 10-, and 16-week old non-mutagenized C3H/HeJ mice

Phenotype	Sex	6-Week Old Mice		10-Week Old Mice		16-Week Old Mice	
		Mean±SD (n=38)	Population Variance (CV)	Mean±SD (n=38-46)	Population Variance (CV)	Mean±SD (n=40)	Population Variance (CV)
Total BMC (mg/mm)	F*	0.78±0.05	6.6	1.05±0.06	5.8	1.31±0.08	5.9
	M	0.94±0.08	8.5	1.28±0.09	7.1	1.59±0.12	7.3
Total BMD (mg/cc)	F	754±17	2.3	889±23	2.6	978±19	1.9
	M	762±15	1.9	884±16	2.0	954±26	2.7
Total Bone Area (mm^2)	F*	1.03±0.09	8.3	1.19±0.09	7.3	1.34±0.07	5.3
	M	1.23±0.09	7.2	1.45±0.10	7.1	1.67±0.10	6.2
Cortical Density (mg/cc)	F	857±23	2.7	979±26	2.7	1060±16	1.5
	M	889±19	2.1	991±18	1.8	1058±21	1.9
Periosteal Circumference (mm)	F*	3.60±0.15	4.1	3.85±0.13	3.1	4.10±0.11	2.6
	M	3.93±0.14	3.6	4.27±0.15	3.6	4.58±0.14	3.0
Endosteal Circumference (mm)	F*	1.52±0.11	7.2	1.40±0.12	8.5	1.34±0.08	6.3
	M	1.76±0.09	5.1	1.63±0.13	8.0	1.64±0.11	6.5

*Male significantly different from female.

Table 4. Correlation coefficients between size sensitive parameters measured by PIXImus and pQCT, before and after adjustment for body weight (n=60).

Phenotype & Measurement Technique	Non-Adjusted Data		Adjusted Data	
	Spearman Correlation Coefficient (r)	p-Value	Spearman Correlation Coefficient (r)	p-Value
	Male/Female			
BMD (PIXImus)	0.65/0.45	<0.0001	<0.02	NS
BMC (PIXImus)	0.74/0.65	<0.0001	<0.02	NS
Bone Area (PIXImus)	0.58/0.62	<0.0001	<0.02	NS
Femur BMD (PIXImus)	0.58//0.63	<0.0001	<0.02	NS
Total CNT (pQCT)	0.70/0.63	<0.0001	<0.02	NS
Total Area (pQCT)	0.65/0.66	<0.0001	<0.02	NS
Periosteal Circumference (pQCT)	0.63/0.63	<0.0001	<0.02	NS
Endosteal Circumference (pQCT)	0.14/0.20	NS		
Cortical Thickness (pQCT)	0.58/0.50	<0.0001	<0.02	NS

Table 5. List of abnormal phenotypes identified in mutagenized C3H/HeJ progeny by dominant (F1) and recessive (F3) screening.

Trait	Phenotype (Mice ID)	Description of Phenotype	Screening Method
<u>Binary</u>	Uncharacterized (Line 2.8.6)	10-12% Low total body BMD, BMC, bone area, & femur BMD, 10-20% low body weight, fur has greasy appearance and increased yellow pigmentation at skin surface	Recessive
Quantitative	Growth (6.5.3)	19% Low body weight	Dominant
	Low BMC, Area, Femur BMD (10.17.7)	20% Low femur BMD, BMC and Bone Area	Dominant
	High BMD & Lean Body Weight (6.9.5)	High lean body weight, high bone mineral content, high bone density	Dominant
	Regional Size (6.5.5)	12% Low bone area at tibia, 4-6% low periosteal circumference	Dominant
	BMC (10.6.6)	Low bone mineral content, low body weight, low periosteal circumference	Recessive
	BMC & IGF-I (Line 6.11.6)	20-25% Low body weight, 30% low IGF-I, 10-13% low bone mineral content	Recessive
	Low Femur BMD (Line 6.5.5)	10% Low femur BMD	Recessive
	BMD (Line 5.27.7)	10-14% Low BMD, low femur BMD, low BMC	Recessive

Table 6. Number of mice tested, phenotypes scored (including visible and musculoskeletal), and inherited mutations identified

Procedure	Number of C3H/HeJ Mice	Number of C57BL/6J Mice
Screened for Dominant Mode of Inheritance	228	452
Screened for Recessive Mode of Inheritance	545	-
Abnormal Phenotypes Identified in Primary Screen (dominant as well as recessive screening)	26	9
Abnormal Phenotypes Confirmed in Secondary Screen	13	5
Phenotypes Introduced to Progeny Testing	13	5
Phenotypes Confirmed in Progeny Testing	4	1
Phenotypes Not-inherited in Progeny Testing (including those died or could not mate)	2	1
Outlier Mice Currently Under Progeny Testing	7	3

Table 7. List of abnormal phenotypes identified in mutagenized C57BL/6J (B6) progeny by dominant (F1) screening.

Phenotype (Mice ID)	Description of Phenotype	Inheritance Test
High lean body mass (9.18.7.A)	20% High lean body mass	Not Confirmed
High BMD (9.18.7.B)	5-7% High BMD at mid-shaft of tibia	Testing
Low Bone Area (9.1.7.A)	17-20% Low BMC, and 10-18% Low bone area at mid-shaft tibia	Confirmed
Decreased serum osteocalcin levels (9.14.6.C)	40-50% Lower serum osteocalcin concentration	Testing
Low Bone Density (9.16.8.C)	4-6% Low Total Body BMD, and 5-7% Low BMD at mid-shaft tibia	Testing

Table 8. Major BMD and soft-tissue regeneration QTLs reported in mouse progenitor strains and corresponding deletion embryonic stem cell clones that are available from The Jackson Laboratory. *Karyotype in progress.

Progenitor Strains Used for Mapping QTL	Chromosomal location	Position (cM)	QTL LOD score	Deletion Map Position (cM)	Deletion Locus Name	ES Clone
C57BL/6 X CAST/EiJ	1	87-95	8.8	67	D1Jcs10	TgN(tkneo)09Jcs
C57BL/6 X C3H/HeJ	1	64-82	24	73*	D1Jcs75	TgN(tkneo)75Jcs
AKR/J X SAMP6	2	2.2-23	4.05	21-24*	D2Jcs37	TgN(tkneo)35Jcs
AKR/J XSAMP6	2	35-45	3.5	38*	D2Jcs24	TgN(tkneo)23Jcs
C57BL/6 X DBA/2	2	45-55		50.3*	D2Jcs46	TgN(tkneo)43Jcs
C57BL/6 X CAST/EiJ	3	0-6.6	5.0			
C57BL/6 X C3H/HeJ	4	35-54	16.3	42.5	D4Jcs7	TgN(tkneo)06Jcs
C57BL/6 X DBA/2	4	60-80	9	65.7*	D4Jcs21	TgN(tkneo)19Jcs
				62.5*	D4Jcs41	TgN(tkneo)39Jcs
C57BL/6 X CAST/EiJ	4	71-76	-			
C57BL/6 X CAST/EiJ	5	25-36	3.6			
C57BL/6 X C3H/HeJ	6	25-36	4.56	29*	D6Jcs25	TgN(tkneo)24Jcs
				34.7*	D6MM5e	TgN(tkneo)60Jcs
SAMP6 X SAMR1	7	11-13	-			
C57BL/6 X DBA/2	7	44				
C57BL/6 X C3H/HeJ	11	49-60	6.76	32*	D11Jcs77	TgN(tkneo)77Jcs
				54*	D11Jcs74	TgN(tkneo)74Jcs
AKR/J X SAMP6	11	49-60	5.4			
SAMP6 X SAMP2	11	58-72	10.0	72*	Fasn	TgN(tkneo)83Jcs
C57BL/6 X CAST/EiJ	13	0-10	6.1	6*	D13Jcs47	TgN(tkneo)44Jcs
				12*	H2b	TgN(tkneo)70Jcs
C57BL/6 X C3H/HeJ	13	35	7.73			
AKR/J X SAMP6	13	22	5.5			
SAMP6 X SAMP2	13	40.4-53.6	-	50*	D13Jcs31	TgN(tkneo)29Jcs
C57BL/6 X C3H/HeJ	14	40	4.3			
C57BL/6 X DBA/2	14	2.0				
C57BL/6 X CAST/EiJ	15	32-49.7	3.2	46*		TgN(tkneo)112Jcs
C57BL/6 X C3H/HeJ	16	27.6	4.07			
AKR/J X SAMP6	16	9-28.4	-	12*	D16Jcs144	TgN(tkneo)144Jcs
C57BL/6 X C3H/HeJ	18	24	13.67			
Soft-Tissue Regeneration QTLs						
MRL/MpJ X SJL/J	1	37-59	7.0			
MRL/MpJ X SJL/J	3	37.2-57.9	6.2	50	D3Jcs26	TgN(tkneo)21Jcs
				52	D3Jcs15	TgN(tkneo)13Jcs
MRL/MpJ X SJL/J	4	3.3-30.6	6.8			
MRL/MpJ X SJL/J	6	17.5-49.2	4.5	29	D6Jcs25	TgN(tkneo)24Jcs
				34.7	D6MM5e	TgN(tkneo)60Jcs
MRL/MpJ X SJL/J	7	26.2-50.3	4.8			
MRL/MpJ X SJL/J	9	31.7-41.5	14.2			
MRL/MpJ X SJL/J	13	32.8-54.6	3.0			

ENU BREEDING SCHEME

♂ +/+ × ♀ +/+ **F0**

ENU Injected Males   Wild Type (WT) Females
(40)   (80)

↓

♀ & ♂   ♀ & ♂   **F1**

+/+   m/+

Non–Affected (99%)   Approximately 1% Mutant
(450)

Recessive Screen

♂   ×   ♀

m/+ or +/+   +/+

F1 (15)   Wild Type (75)

↓

♀   ×   ♂   **F2**

+/+   m/+ or +/+

225 F2   15 F1

↓

♀ & ♂   ♀ & ♂   ♀ & ♂   **F3**

m/m   m/+   +/+

25%   50%   25%

280   560   280
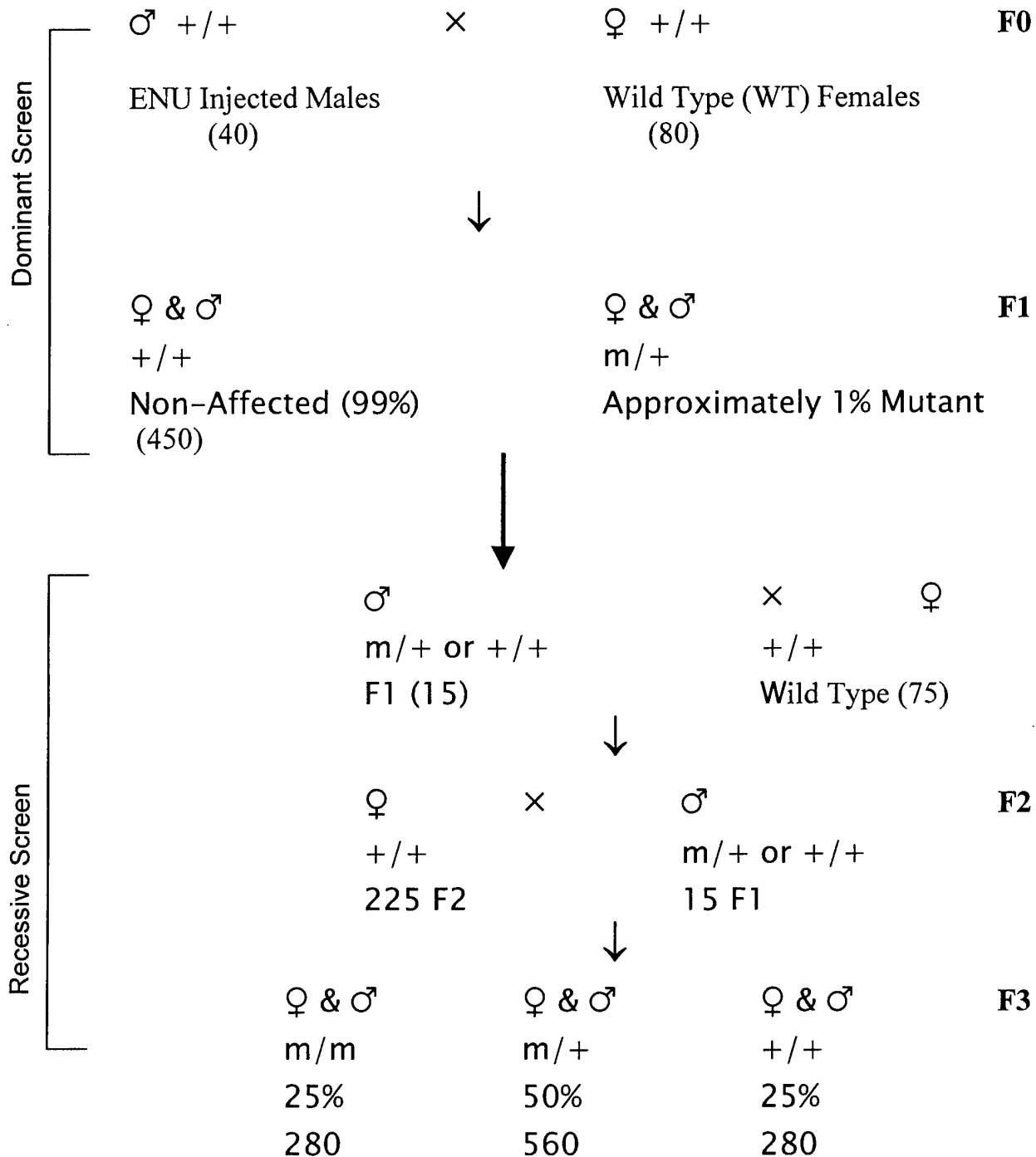
Figure 1. ENU Breeding Scheme. The breeding scheme incorporates both dominant and recessive screens. We have screened about 230 C3H/HeJ mice for dominant screen and about 550 mice in recessive screen.
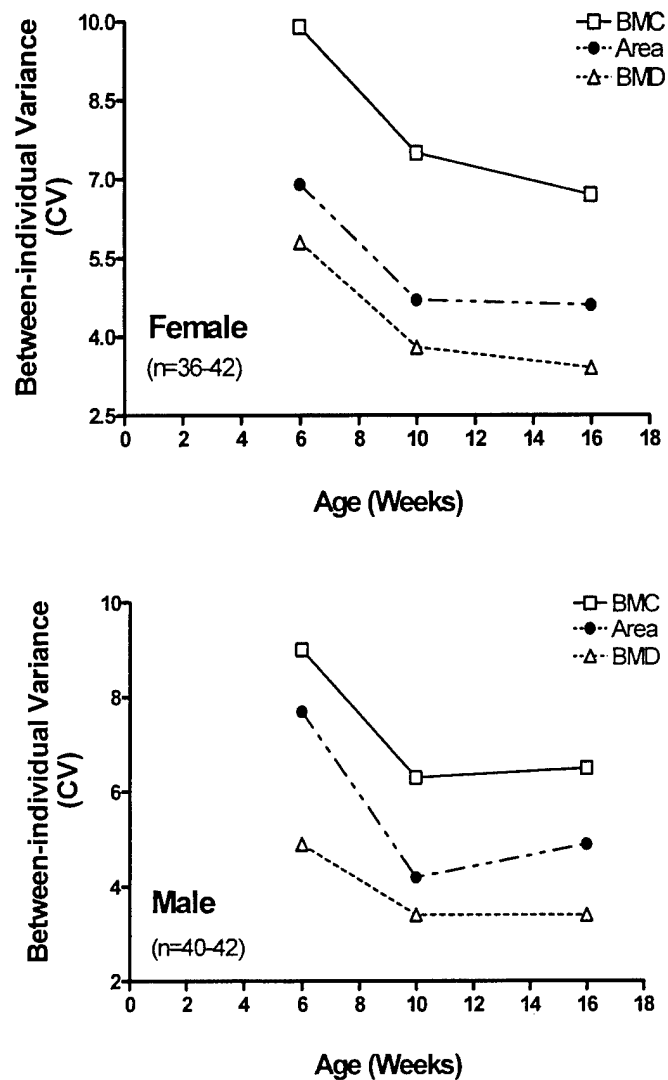
Figure 2. Population variance in the measurements of bone mineral density, bone mineral content, and bone area as determined by Dual Energy X-ray Absorptiometry (DEXA) of female and male C3H/HeJ mice. The higher CVs at 6-week age would result in classification errors in identifying abnormal phenotype using this technique.
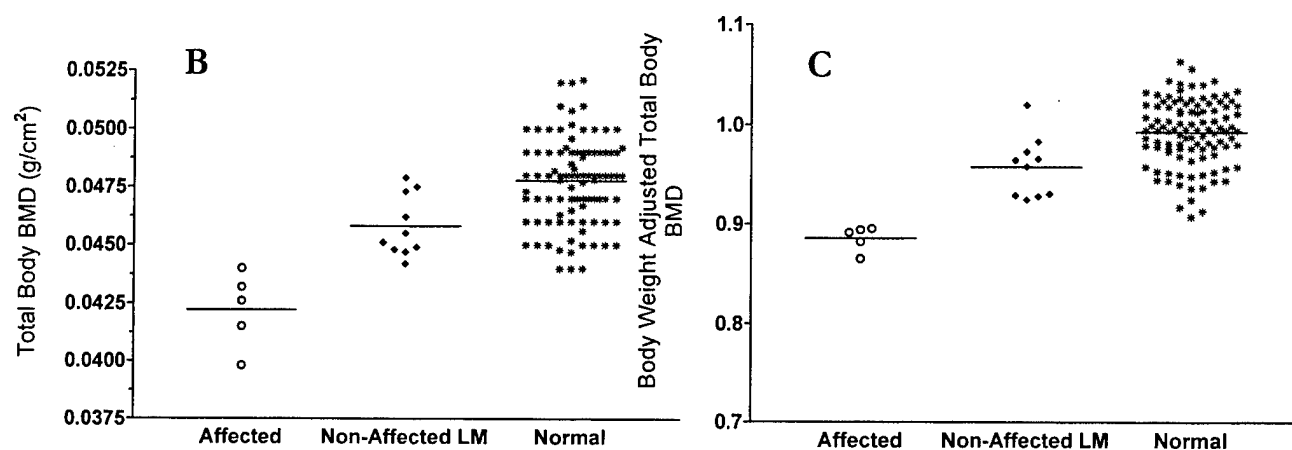
Figure 3. Mutant mice with visible phenotypes detected in F3 progeny in recessive screen. (A) A yet to be fully characterized mutant mice (Right) shown with normal littermate (Left), affected mice appears weak (low body weight) and shows fur with greasy appearance early in development (birth to 6-week age). Adults have hairs with increased yellow pigmentation, and low BMD (B & C).
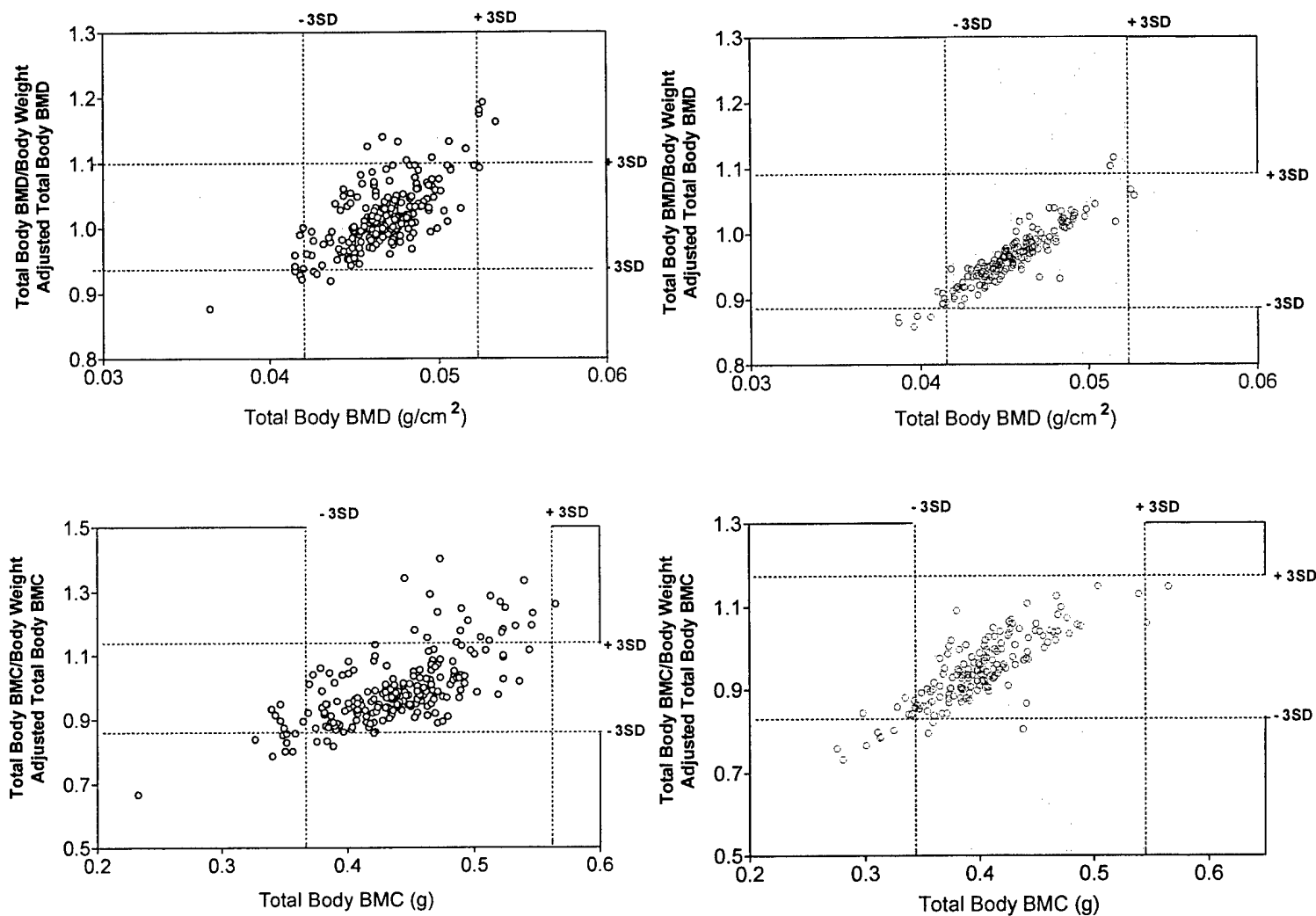
Figure 4. Representative data on body-weight-adjusted and non-adjusted BMD and BMC from 400 F3 progeny screened for BMD and BMC. The 3SD values were calculated from normal 10-week old male (n=60) and female (n=60) C3H mice. Outlier were identified as those having both adjusted and non-adjusted values outside the 3SD range.
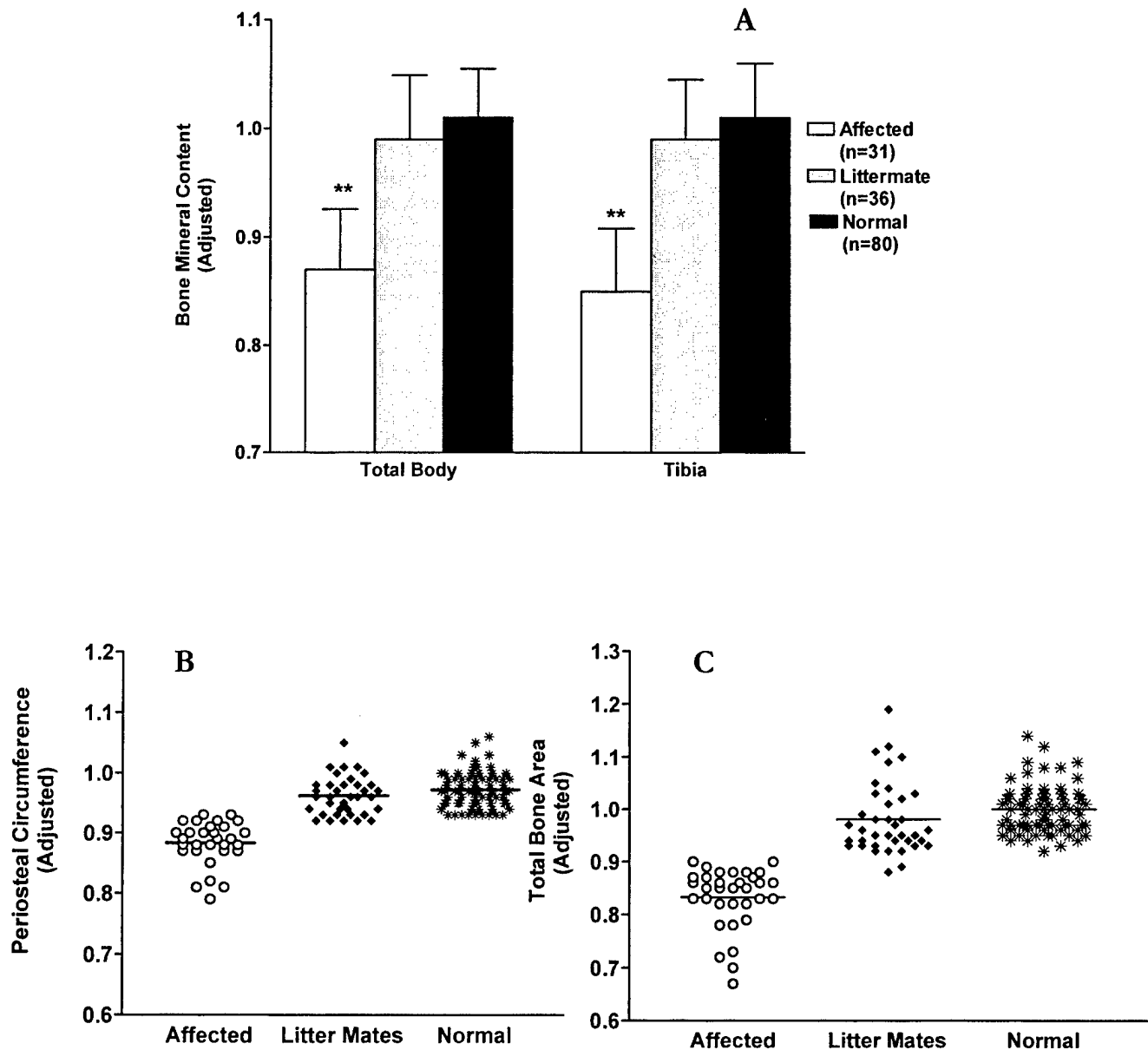
*Figure 5. Phenotype of 16-week old inheritance test progeny from a C3H phenodeviant (5.37.5) identified with low bone mineral content in dominant screening. (A) The body weight adjusted total BMC measured by DEXA was 12% lower and BMC at mid shaft tibia measured by pQCT was 14% lower in the affected (n=31) progeny as compared with non-affected littermates (n=36) or normal non-mutagenized mice (n=80). The unadjusted BMC was about 20% lower in affected progeny at both sites. In addition, the body weight adjusted periosteal circumference (B) and total body bone area (A) were significantly (p<0.0001) decreased in affected progeny as compared to littermate. This suggests that this phenodeviant has a mutation that is affecting bone size at multiple skeletal sites. **p<0.0001.*
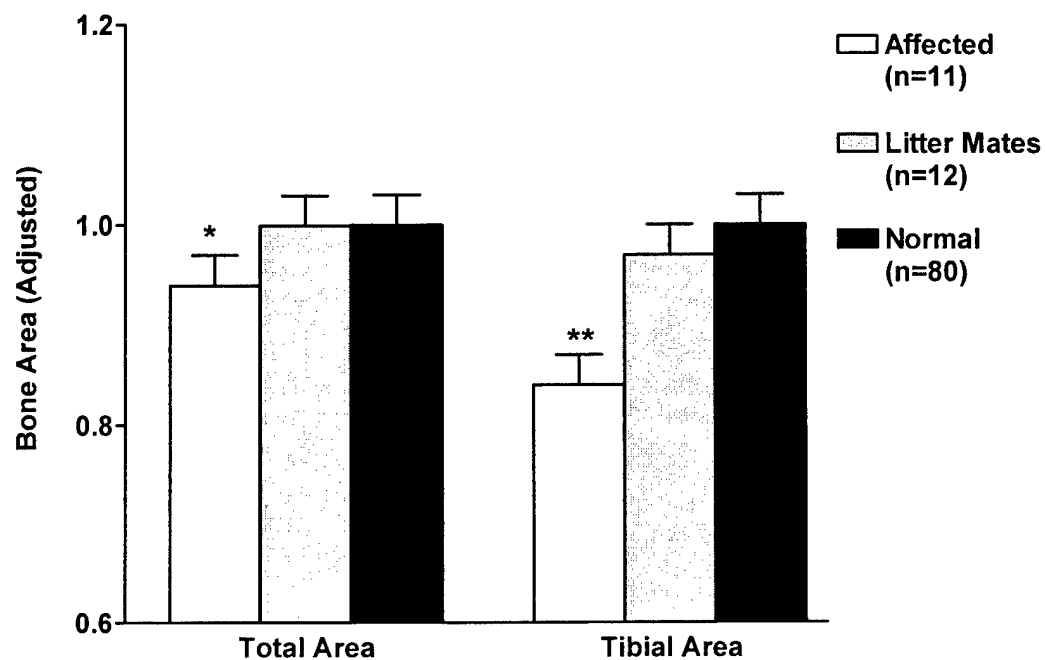
*Figure 6. Phenotype of 16-week old inheritance test progeny from a C3H phenodeviant (6.5.5) identified as low bone size in dominant screening. The affected progeny shows larger decrease in bone area (-12%, p<0.0001) at mid shaft tibia as compared to a lower decrease of 6% (p<0.05) in total body bone area. The BMD was not significantly different in affected progeny as compared to non-affected littermate or non-mutagenized normal. The larger effect in tibia shows that this mutation has different magnitude of effect at different skeletal sites. *p<0.05, **p<0.0001*
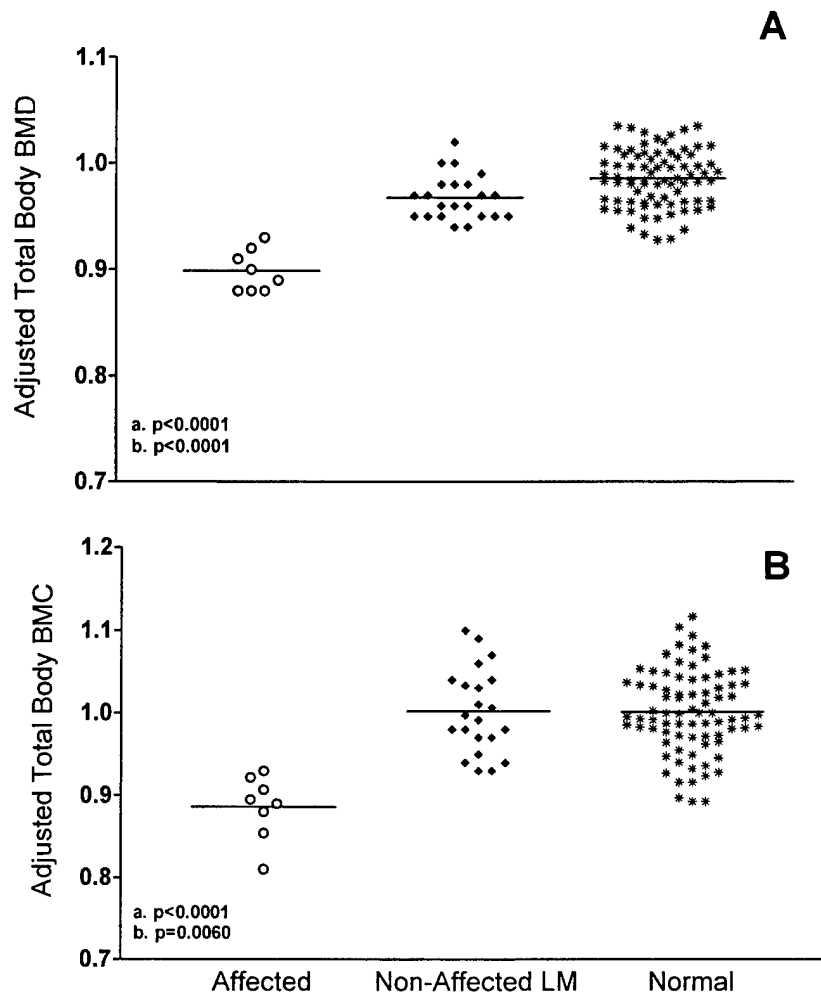
Figure 7. Phenotype of 16-week old progeny from a C3H phenodeviant (5.27.7) identified in recessive screen. Body weight adjusted total body bone density was 8-10% lower in affected (n=8) progeny are compared with non-affected littermates (n=23) and normal non-mutagenized control mice (n=80). In addition, the affected mice had 18% lower BMC and no change in bone area. The femur BMD measured by DEXA and tibia BMD measured at mid shaft tibia were also lower by 10% (p<0.001) and 3% (p<0.05), respectively. The data indicates that mutation is affecting bone density at multiple skeletal sites. a = p-value between affected and non-affected litter mates, b = p-value between affected and normal mice.
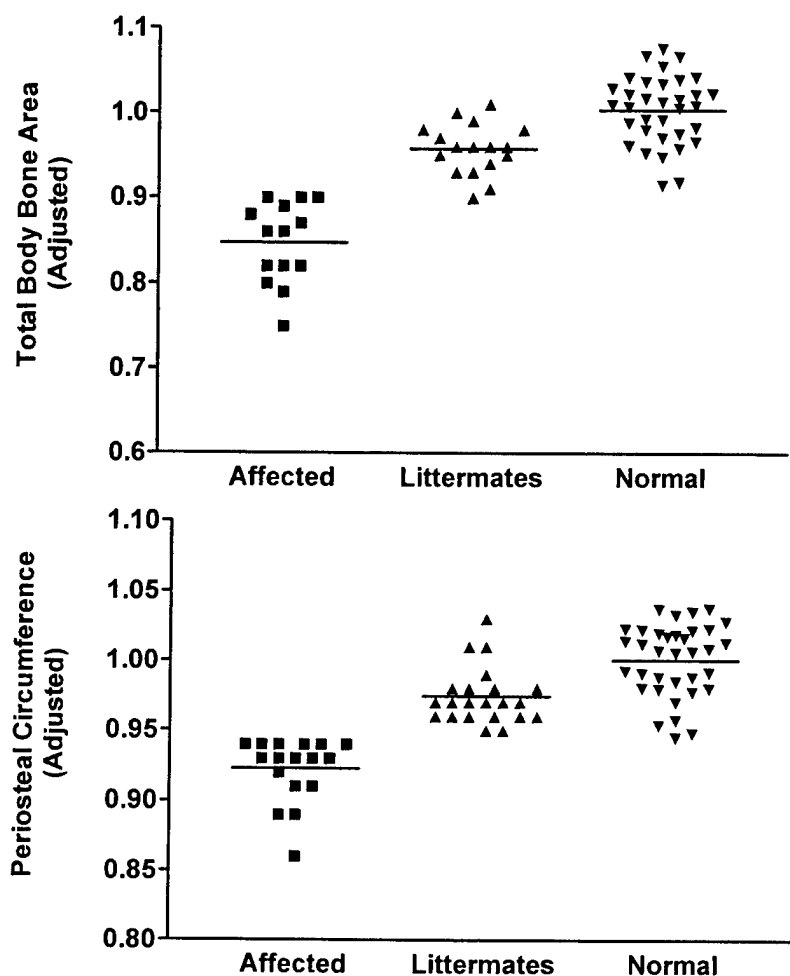
Figure 8. Phenotype of 16-week old progeny from an outlier mice (9.1.7) identified in B6 dominant screen. Mean body weight adjusted total body bone area was 16% lower (p<0.0001) in affected (n=17) progeny are compared with non-affected littermates (n=23) and normal non-mutagenized control mice (n=80). In addition, the affected mice had 6% (p<0.05) lower periosteal circumference at mid shaft tibia. The data indicates that mutation is affecting bone size at multiple skeletal sites.